regarded as a potential target for cancer therapy. Suppression of nSMase2 expression in cancer cells by RNAi technology or using a specific chemical inhibitor, such as GW4869, may provide therapeutic benefit. However, we should be careful about the possible side effects because nSMase2 is involved in a wide range of physiological events, and its deficiency may lead to diseases (Stoffel et al., 2005; Tabatadze et al., 2010; Poirier et al., 2012). In addition to secretory mechanisms, elucidation of the exosomal miRNA-sorting mechanisms will also benefit cancer therapy. If specific molecules recruit oncogenic miRNAs into tumor cell-derived exosomes, such molecules will be a novel target for cancer therapy. Furthermore, several groups have reported that miRNAs can exist in the extracellular space without exosome encapsulation (Kosaka et al., 2013b). In these cases, miRNAs are secreted in association with the RISC effector Ago2 (Arroyo et al., 2011, Turchinovich et al., 2011) or high-/low-density lipoprotein (Vickers et al., 2011). Interestingly, a latest study has reported that EBV-derived miR-BART17 is co-purified with a protein-rich fraction but not with exosomes, whereas miRNA-16 originated from cells is mainly co-purified with the exosome fraction (Gourzones et al., 2013). These exosome-free extracellular miRNAs may also be therapeutic targets, although their biological significance has not yet been documented. In summary, this research field holds great promise for the development of cancer therapies, but extensive further studies are required, especially to elucidate the basic mechanisms underlying the biosynthesis, sorting, and secretion of exosomal miRNAs.

The other possibility for clinical application of this research field is to utilize exosomal miRNAs as drugs. The findings that exosomal miRNAs secreted from MSCs promote tissue repair indicate their potential application for cell-free regenerative medicine. The feasibility of this approach is further supported by the fact that MSCs can be isolated from patients without immunological rejection, and they can be readily expanded many-fold *in vitro*. However, we still must be careful about the safety issues because exosomes contain a wide range of molecules, and it is hard to predict the overall outcome of MSC-derived exosome administration. In particular, we caution that exosomes with tissue-repair effects may serve as an oncogenic factor when non-specifically delivered to uninjured tissue. Thus, it is essential to develop technologies to deliver therapeutic exosomes specifically to target tissue. If surface molecules expressed on the target tissue are known, surface modification of the exosomes will improve the efficiency of specific delivery (Alvarez-Erviti et al., 2011; Ohno et al., 2013). Another potential strategy is the utilization of MSCs as a vehicle for the delivery of exosomal miRNAs. This concept is based on the mouse study by Pan et al., in which it was shown that intrasplenically transplanted Huh7 cells transduced with CD81 shRNA can efficiently deliver functional CD81 siRNA to recipient hepatocytes via exosome transfer (Pan et al., 2011). Because MSCs can be directed and engrafted to injured sites (Chamberlain et al., 2007), the systemic administration of MSCs that have been genetically modified to overexpress therapeutic miRNAs might enable more efficient delivery of exosomal miRNAs than direct exosome administration. Furthermore, if the understanding of exosome secretion mechanisms in MSCs becomes clear, genetic modification of MSCs to increase exosome secretion may enhance the therapeutic feasibility.

In conclusion, research on exosomal miRNAs is now unveiling a variety of biological phenomena whose mechanisms are not yet clear. Furthermore, this research field holds great promise for therapeutic applications, including cancer therapy and regenerative medicine. However, to realize the clinical application, it is necessary to elucidate the fundamental biology of this field, including the mechanisms underlying biogenesis, sorting, and secretion of exosomal miRNAs. Furthermore, we must always be careful about safety issues before clinical applications.

Acknowledgments: This work was supported in part by a Grant-in-Aid for the Third-Term Comprehensive 10-Year Strategy for Cancer Control; a Grant-in-Aid for Scientific Research on Priority Areas Cancer from the Ministry of Education, Culture, Sports, Science and Technology; the Program for Promotion of Fundamental Studies in Health Sciences of the National Institute of Biomedical Innovation (NiBio); the Japan Society for the Promotion of Science (JSPS) through the 'Funding Program for World-Leading Innovative R&D on Science and Technology (FIRST Program)', initiated by the Council for Science and Technology Policy (CSTP); a Grant-in-Aid for Scientific Research on Innovative Areas ('functional machinery for non-coding RNAs') from the Japanese Ministry of Education, Culture, Sports, Science, and Technology; and the Comprehensive Research and Development of a Surgical Instrument for Early Detection and Rapid Curing of Cancer Project (P10003) of the New Energy and Industrial Technology Development Organization (NEDO).

Received July 16, 2013; accepted December 4, 2013; previously published online December 9, 2013

References

Alvarez-Erviti, L., Seow, Y., Yin, H., Betts, C., Lakhal, S., and Wood, M.J. (2011). Delivery of siRNA to the mouse brain by systemic injection of targeted exosomes. Nat. Biotechnol. *29*, 341–345.

Arroyo, J.D., Chevillet, J.R., Kroh, E.M., Ruf, I.K., Pritchard, C.C., Gibson, D.F., Mitchell, P.S., Bennett, C.F., Pogosova-Agadjanyan, E.L., Stirewalt, D.L., et al. (2011). Argonaute2 complexes carry a population of circulating microRNAs independent of vesicles in human plasma. Proc. Natl. Acad. Sci. USA *108*, 5003–5008.

Bartel, D.P. (2009). MicroRNAs: target recognition and regulatory functions. Cell *136*, 215–233.

Camacho, L., Guerrero, P., and Marchetti, D. (2013). MicroRNA and protein profiling of brain metastasis competent cell-derived exosomes. PLoS One *8*, e73790.

Chamberlain, G., Fox, J., Ashton, B., and Middleton, J. (2007). Concise review: mesenchymal stem cells: their phenotype, differentiation capacity, immunological features, and potential for homing. Stem Cells *25*, 2739–2749.

Chen, T.S., Lai, R.C., Lee, M.M., Choo, A.B., Lee, C.N., and Lim, S.K. (2010). Mesenchymal stem cell secretes microparticles enriched in pre-microRNAs. Nucleic Acids Res. *38*, 215–224.

Chitwood, D.H. and Timmermans, M.C. (2010). Small RNAs are on the move. Nature *467*, 415–419.

Collino, F., Deregibus, M.C., Bruno, S., Sterpone, L., Aghemo, G., Viltono, L., Tetta, C., and Camussi, G. (2010). Microvesicles derived from adult human bone marrow and tissue specific mesenchymal stem cells shuttle selected pattern of miRNAs. PLoS One *5*, e11803.

Delorme-Axford, E., Donker, R.B., Mouillet, J.F., Chu, T., Bayer, A., Ouyang, Y., Wang, T., Stolz, D.B., Sarkar, S.N., Morelli, A.E., et al. (2013). Human placental trophoblasts confer viral resistance to recipient cells. Proc. Natl. Acad. Sci. USA *110*, 12048–12053.

Gesierich, S., Berezovskiy, I., Ryschich, E., and Zöller, M. (2006). Systemic induction of the angiogenesis switch by the tetraspanin D6.1A/CO-029. Cancer Res. *66*, 7083–7094.

Gourzones, C., Ferrand, F.R., Amiel, C., Vérillaud, B., Barat, A., Guérin, M., Gattolliat, C.H., Gelin, A., Klibi, J., Chaaben, A.B., et al. (2013). Consistent high concentration of the viral microRNA BART17 in plasma samples from nasopharyngeal carcinoma patients – evidence of non-exosomal transport. Virol. J. *10*, 119.

Grange, C., Tapparo, M., and Collino, F. (2011). Microvesicles released from human renal cancer stem cells stimulate angiogenesis and formation of lung premetastatic niche microvesicles released from human renal cancer stem. Cancer Res. *71*, 5346–5356.

Gu, Y., Li, M., Wang, T., Liang, Y., Zhong, Z., Wang, X., Zhou, Q., Chen, L., Lang, Q., He, Z., et al. (2012). Lactation-related MicroRNA expression profiles of porcine breast milk exosomes. PLoS One *7*, e43691.

Higginbotham, J.N., Demory Beckler, M., Gephart, J.D., Franklin, J.L. Bogatcheva, G., Kremers, G.J., Piston, D.W., Ayers, G.D., McConnell, R.E., Tyska, M.J., et al. (2011). Amphiregulin exosomes increase cancer cell invasion. Curr. Biol. *21*, 779–786.

Hsu, C., Morohashi, Y., Yoshimura, S., Manrique-Hoyos, N., Jung, S., Lauterbach, M.A., Bakhti, M., Grønborg, M., Möbius, W., Rhee, J., et al. (2010). Regulation of exosome secretion by Rab35 and its GTPase-activating proteins TBC1D10A-C. J. Cell Biol. *189*, 223–132.

Hwang, I., Shen, X., and Sprent, J. (2003). Direct stimulation of naive T cells by membrane vesicles from antigen-presenting cells: distinct roles for CD54 and B7 molecules. Proc. Natl. Acad. Sci. USA *100*, 6670–6675.

Jung, T., Castellana, D., Klingbeil, P., Cuesta Hernández, I., Vitacolonna, M., Orlicky, D.J., Roffler, S.R., Brodt, P., and Zöller, M. (2009). CD44v6 dependence of premetastatic niche preparation by exosomes. Neoplasia *11*, 1093–1105.

Katsuda, T., Kosaka, N., Takeshita, F., and Ochiya, T. (2013). The therapeutic potential of mesenchymal stem cell-derived extracellular vesicles. Proteomics *13*, 1637–1653.

Kogure, T., Lin, W.L., Yan, I.K., Braconi, C., and Patel, T. (2011). Intercellular nanovesicle mediated microRNA transfer: a mechanism of environmental modulation of hepatocellular cancer cell growth. Hepatology *54*, 1237–1248.

Kosaka, N. and Ochiya, T. (2011). Unraveling the mystery of cancer by Secretory microRNA: horizontal microRNA transfer between living cells. frontiers in genetics. Front. Genet. *2*, 97.

Kosaka, N., Iguchi, H., and Ochiya, T. (2010a). Circulating microRNA in body fluid: a new potential biomarker for cancer diagnosis and prognosis. Cancer Sci. *101*, 2087–2092.

Kosaka, N., Iguchi, H., Yoshioka,Y., Takeshita, F., Matsuki, Y., and Ochiya, T. (2010b). Secretory mechanisms and intercellular transfer of microRNAs in living cells. J. Biol. Chem. *285*, 17442–17452.

Kosaka, N., Izumi, H., Sekine, K., and Ochiya, T. (2010c). MicroRNA as a new immune-regulatory agent in breast milk. Silence *1*, 7.

Kosaka, N., Iguchi, H., Yoshioka, Y., Hagiwara, K., Takeshita, F., and Ochiya, T. (2012). Competitive interactions of cancer cells and normal cells via secretory microRNAs. J. Biol. Chem. *287*, 1397–1405.

Kosaka, N., Iguchi, H., Hagiwara, K., Yoshioka, Y., Takeshita, F., and Ochiya, T. (2013a). Neutral sphingomyelinase 2 (nSMase2)-dependent exosomal transfer of angiogenic microRNAs regulate cancer cell metastasis. J. Biol. Chem. *288*, 10849–10859.

Kosaka, N., Yoshioka, Y., Hagiwara, K., Tominaga, N., Katsuda, T., and Ochiya T. (2013b). Trash or treasure: extracellular microRNAs and cell-to-cell communication. Front. Genet. *4*, 173.

Kwak, P.B., Iwasaki, S., and Tomari, Y. (2010). The microRNA pathway and cancer. Cancer Sci. *101*, 2309–2315.

Lagos-Quintana, M., Rauhut, R., Lendeckel, W., and Tuschl, T. (2001). Identification of novel genes coding for small expressed RNAs. Science *294*, 853–858.

Lawrie, C.H., Gal, S., Dunlop, H.M., Pushkaran, B., Liggins, A.P., Pulford, K., Banham, A.H., Pezzella, F., Boultwood, J., Wainscoat, J.S., et al. (2008). Detection of elevated levels of tumour-associated microRNAs in serum of patients with diffuse large B-cell lymphoma. Br. J. Haematol. *141*, 672–675.

Lee, R.C., Feinbaum, R.L., and Ambros, V. (1993). The C. elegans heterochronic gene lin-4 encodes small RNAs with antisense complementarity to lin-14. Cell *75*, 843–854.

Lewis, B.P., Burge, C.B., and Bartel, D.P. (2005). Conserved seed pairing, often flanked by adenosines, indicates that thousands of human genes are microRNA targets. Cell *120*, 15–20.

Mitchell, P.S., Parkin, R.K., Kroh, E.M., Fritz, B.R., Wyman, S.K., Pogosova-Agadjanyan, E.L., Peterson, A., Noteboom, J., O'Briant, K.C., Allen, A., et al. (2008). Circulating microRNAs as stable blood-based markers for cancer detection. Proc. Natl. Acad. Sci. USA *105*, 10513–10518.

Mittelbrunn, M., Gutiérrez-Vázquez, C., Villarroya-Beltri, C., González, S., Sánchez-Cabo, F., González, M.Á., Bernad, A., and Sánchez-Madrid, F. (2011). Unidirectional transfer of microRNA-loaded exosomes from T cells to antigen-presenting cells. Nat. Commun. *2*, 282.

Montecalvo, A., Larregina, A.T., Shufesky, W.J., Stolz, D.B., Sullivan, M.L.G., Karlsson, J.M., Baty, C.J., Gibson, G.A., Erdos, G., Wang, Z., et al. (2012). Mechanism of transfer of functional microRNAs between mouse dendritic cells via exosomes. Blood *119*, 756–766.

Munch, E.M., Harris, R.A., Mohammad, M., Benham, A.L., Pejerrey, S.M., Showalter, L., Hu, M., Shope, C.D., Maningat, P.D., Gunaratne, P.H., et al. (2013). Transcriptome profiling of microRNA by next-gen deep sequencing reveals known and novel miRNA species in the lipid fraction of human breast milk. PLoS One *8*, e50564.

Ohno, S., Takanashi, M., Sudo, K., Ueda, S., Ishikawa, A., Matsuyama, N., Fujita, K., Mizutani, T., Ohgi, T., Ochiya, T., et al. (2013). Systemically injected exosomes targeted to EGFR deliver antitumor microRNA to breast cancer cells. Mol. Ther. *21*, 185–191.

Ostrowski, M., Carmo, N.B., Krumeich, S., Fanget, I., Raposo, G., Savina, A., Moita, C.F., Schauer, K., Hume, A.N., Freitas, R.P., et al. (2010). Rab27a and Rab27b control different steps of the exosome secretion pathway. Nat. Cell Biol. *12*, 19–30.

Pan, Q., Ramakrishnaiah, V., Henry, S., Fouraschen, S., de Ruiter, P.E., Kwekkeboom, J., Tilanus, H.W., Janssen, H.L., and van der Laan, L.J. (2011). Hepatic cell-to-cell transmission of small silencing RNA can extend the therapeutic reach of RNA interference (RNAi). Gut *61*, 1330–1339.

Pegtel, D.M., Cosmopoulos, K., Thorley-Lawson, D.A., van Eijndhoven, M.A., Hopmans, E.S., Lindenberg, J.L., de Gruijl, T.D., Würdinger, T., and Middeldorp, J.M. (2010). Functional delivery of viral miRNAs via exosomes. Proc. Natl. Acad. Sci. USA *107*, 6328–6333.

Peinado, H., Alečković, M., Lavotshkin, S., Matei, I., Costa-Silva, B., Moreno-Bueno, G., Hergueta-Redondo, M., Williams, C., García-Santos, G., Ghajar, C., et al. (2012). Melanoma exosomes educate bone marrow progenitor cells toward a pro-metastatic phenotype through MET. Nat. Med. *18*, 883–891.

Poirier, C., Berdyshev, E.V., Dimitropoulou, C., Bogatcheva, N.V., Biddinger, P.W., and Verin, A.D. (2012). Neutral sphingomyelinase 2 deficiency is associated with lung anomalies similar to emphysema. Mamm. Genome *23*, 758–763.

Ramakrishnaiah, V., Thumann, C., Fofana, I., Habersetzer, F., Pan, Q., de Ruiter, P.E., Willemsen, R., Demmers, J.A., Stalin Raj, V., Jenster, G., et al. (2013). Exosome-mediated transmission of hepatitis C virus between human hepatoma Huh7.5 cells. Proc. Natl. Acad. Sci. USA *110*, 13109–13113.

Rana, S., Malinowska, K., and Zöller, M. (2013). Exosomal tumor MicroRNA modulates premetastatic organ cells. Neoplasia *15*, 281–295.

Raposo, G., Nijman, H.W., Stoorvogel, W., Liejendekker, R., Harding, C.V, Melief, C.J.M., and Geuze, H.J. (1996). B lymphocytes secrete antigen-presentingvesicles. J. Exp. Med. *183*, 1161–1172.

Ratajczak, J., Miekus, K., Kucia, M., Zhang, J., Reca, R., Dvorak, P., and Ratajczak, M.Z. (2006). Embryonic stem cell-derived microvesicles reprogram hematopoietic progenitors: evidence for horizontal transfer of mRNA and protein delivery. Leukemia *20*, 847–856.

Reinhart, B.J., Weinstein, E.G., Rhoades, M.W., Bartel, B., and Bartel, D.P. (2002). MicroRNAs in plants. Genes Dev. *16*, 1616–1626.

Roccaro, A.M., Sacco, A., Maiso, P., Azab, A.K., Tai, Y., Reagan, M., Azab, F., Flores, L.M., Campigotto, F., Weller, E., et al. (2013). BM mesenchymal stromal cell-derived exosomes facilitate multiple myeloma progression. J. Clin. Invest. *123*, 1542–1555.

Skog, J., Würdinger, T., van Rijn, S., Meijer, D.H., Gainche, L., Sena-Esteves, M., Curry, W.T. Jr., Carter, B.S., Krichevsky, A.M., and Breakefield, X.O. (2008). Glioblastoma microvesicles transport RNA and proteins that promote tumour growth and provide diagnostic biomarkers. Nat. Cell Biol. *10*, 1470–1476.

Skokos, D., Le Panse, S., Villa, I., Rousselle, J. C., Peronet, R., David, B., Namane, A., and Mécheri, S. (2001). Mast cell-dependent B and T lymphocyte activation is mediated by the secretion of immunologically active exosomes. J. Immunol. *166*, 868–876.

Skokos, D., Botros, H.G., Demeure, C., Morin, J., Peronet, R., Birkenmeier, G., Boudaly, S., and Mécheri, S. (2003). Mast cell-derived exosomes induce phenotypic and functional maturation of dendritic cells and elicit specific immune responses *in vivo*. J. Immunol. *170*, 3037–3045.

Stoffel, W., Jenke, B., Blöck, B., Zumbansen, M., and Koebke, J. (2005). Neutral sphingomyelinase 2 (smpd3) in the control of postnatal growth and development. Proc. Natl. Acad. Sci. USA *102*, 4554–4559.

Sun, Q., Chen, X., Yu, J., Zen, K., Zhang, C.Y., and Li, L. (2013). Immune modulatory function of abundant immune-related microRNAs in microvesicles from bovine colostrum. Protein Cell. *4*, 197–210.

Tabatadze, N., Savonenko, A., Song, H., Bandaru, V.V., Chu, M., and Haughey, N.J. (2010). Inhibition of neutral sphingomyelinase-2 perturbs brain sphingolipid balance and spatial memory in mice. J. Neurosci. Res. *88*, 2940–2451.

Tadokoro, H., Umezu, T., Ohyashiki, K., Hirano, T., and Ohyashiki, J.H. (2013). Exosomes derived from hypoxic leukemia cells enhance tube formation in endothelial cells. J. Biol. Chem. *288*, 34343–34351.

Taylor, D.D. and Gercel-Taylor, C. (2008). MicroRNA signatures of tumor-derived exosomes as diagnostic biomarkers of ovarian cancer. Gynecol. Oncol. *110*, 13–21.

Théry, C. (2011). Exosomes: secreted vesicles and intercellular communications. F1000 Biol. Rep. *3*, 15.

Thompson, C.A., Purushothaman, A., Ramani, V.C., Vlodavsky, I., and Sanderson, R.D. (2013). Heparanase regulates secretion, composition and function of tumor cell-derived exosomes. J. Biol. Chem. *288*, 10093–10099.

Trajkovic, K., Hsu, C., Chiantia, S., Rajendran, L., Wenzel, D., Wieland, F., Schwille, P., Brügger, B., and Simons, M. (2008). Ceramide triggers budding of exosome vesicles into multivesicular endosomes. Science *319*, 1244–1247.

Turchinovich, A., Weiz, L., Langheinz, A., and Burwinkel, B. (2011). Characterization of extracellular circulating microRNA. Nucleic Acids Res. *39*, 7223–7233.

Valadi, H., Ekström, K., Bossios, A., Sjöstrand, M., Lee, J.J., and Lötvall, J.O. (2007). Exosome-mediated transfer of mRNAs and

microRNAs is a novel mechanism of genetic exchange between cells. Nat. Cell Biol. *9*, 654–659.

Vickers, K.C., Palmisano, B.T., Shoucri, B.M., Shamburek, R.D., and Remaley, A.T. (2011). MicroRNAs are transported in plasma and delivered to recipient cells by high-density lipoproteins. Nat. Cell Biol. *13*, 423–433.

Weber, J.A., Baxter, D.H., Zhang, S., Huang, D.Y., Huang, K.H., Lee, M.J., Galas, D.J., and Wang, K. (2010). The microRNA spectrum in 12 body fluids. Clin. Chem. *56*, 1733–1741.

Xin, H., Li, Y., Buller, B., Katakowski, M., Zhang, Y., Wang, X., Shang, X., Zhang, Z.G., and Chopp, M. (2012). Exosome-mediated transfer of miR-133b from multipotent mesenchymal stromal cells to neural cells contributes to neurite outgrowth. Stem Cells *30*, 1556–1564.

Xin, H., Li, Y., Liu, Z., Wang, X., Shang, X., Cui, Y., Gang Zhang, Z., and Chopp, M. (2013). Mir-133b promotes neural plasticity and functional recovery after treatment of stroke with multipotent mesenchymal stromal cells in rats via transfer of exosome-enriched extracellular particles. Stem Cells *31*, 2737–2746.

Yamada, N., Nakagawa, Y., Tsujimura, N., Kumazaki, M., Noguchi, S., Mori, T., Hirata, I., Maruo, K., and Akao, Y. (2013). Role of intracellular and extracellular microRNA-92a in colorectal cancer. Transl. Oncol. *6*, 482–492.

Yu, B., Gong, M., Wang, Y., Millard, R.W., Pasha, Z., Yang, Y., Ashraf, M., and Xu, M. (2013). Cardiomyocyte protection by GATA-4 gene engineered mesenchymal stem cells is partially mediated by translocation of miR-221 in microvesicles. PLoS One *8*, e73304.

Zhang, Y., Liu, D., Chen, X., Li, J., Li, L., Bian, Z., Sun, F., Lu, J., Yin, Y., Cai, X., et al. (2010). Secreted monocytic miR-150 enhances targeted endothelial cellmigration. Mol. Cell. *39*, 133–144.

Zhou, Q., Li, M., Wang, X., Li, Q., Wang, T., Zhu, Q., Zhou, X., Wang, X., Gao, X., and Li, X. (2012). Immune-related microRNAs are abundant in breast milk exosomes. Int. J. Biol. Sci. *8*, 118–123.

Zitvogel, L., Regnault, A., Lozier, A., Wolfers, J., Flament, C., Tenza, D., Ricciardi-Castagnoli, P., Raposo, G., and Amigorena, S. (1998). Eradication of established murine tumors using a novel cell-free vaccine: dendritic cell derived exosomes. Nat. Med. *4*, 594–660.

CANCER

Exosomes from bone marrow mesenchymal stem cells contain a microRNA that promotes dormancy in metastatic breast cancer cells

Makiko Ono,[1] Nobuyoshi Kosaka,[1] Naoomi Tominaga,[1] Yusuke Yoshioka,[1] Fumitaka Takeshita,[1] Ryou-u Takahashi,[1] Masayuki Yoshida,[2] Hitoshi Tsuda,[3] Kenji Tamura,[4] Takahiro Ochiya[1]*

Breast cancer patients often develop metastatic disease years after resection of the primary tumor. The patients are asymptomatic because the disseminated cells appear to become dormant and are undetectable. Because the proliferation of these cells is slowed, dormant cells are often unresponsive to traditional chemotherapies that exploit the rapid cell cycling of most cancer cells. We generated a bone marrow–metastatic human breast cancer cell line (BM2) by tracking and isolating fluorescent-labeled MDA-MB-231 cells that disseminated to the bone marrow in mice. Coculturing BM2 cells with bone marrow mesenchymal stem cells (BM-MSCs) isolated from human donors revealed that BM-MSCs suppressed the proliferation of BM2 cells, decreased the abundance of stem cell–like surface markers, inhibited their invasion through Matrigel Transwells, and decreased their sensitivity to docetaxel, a common chemotherapy agent. Acquisition of these dormant phenotypes in BM2 cells was also observed by culturing the cells in BM-MSC–conditioned medium or with exosomes isolated from BM-MSC cultures, which were taken up by BM2 cells. Among various microRNAs (miRNAs) increased in BM-MSC–derived exosomes compared with those from adult fibroblasts, overexpression of miR-23b in BM2 cells induced dormant phenotypes through the suppression of a target gene, *MARCKS*, which encodes a protein that promotes cell cycling and motility. Metastatic breast cancer cells in patient bone marrow had increased *miR-23b* and decreased *MARCKS* expression. Together, these findings suggest that exosomal transfer of miRNAs from the bone marrow may promote breast cancer cell dormancy in a metastatic niche.

INTRODUCTION

Breast cancer is the most common cancer; about 70,000 cases were newly diagnosed in 2010, with more than 12,000 deaths reported in 2012 in Japan (*1*). Although breast cancer mortality in Western countries is decreasing because of early detection and effective systemic adjuvant therapy, breast cancer recurrence often occurs, typically within 5 years but even up to 10 to 20 years after surgery (*2*). Because recurrence is often more aggressive and untreatable, it is important to identify the mechanisms that enable therapeutic subversion and regrowth. This phenomenon indicates that breast cancer cells survive for a long time somewhere in the body in a state of cancer dormancy, in which cells cease dividing but survive in a quiescent state while waiting for appropriate environmental conditions to begin proliferation again. Clinical reports show that disseminated breast cancer cells can be detected in the bone marrow (BM) at early stages of breast cancer and is a strong prognostic factor (*3*). Bone marrow is a common homing tissue for disseminated tumor cells, many of which have surface abundance of CD44 but not CD24 ($CD44^+$ and $CD24^-$), a characteristic common to breast cancer stem cells (CSCs) (*4*). It is thought that micrometastases form in the bone marrow and then recirculate to invade other, distant organs (*5*).

By contrast, hematopoietic stem cells, which have the properties of self-renewal and pluripotency, are thought to be regulated by signals derived from the bone marrow microenvironment, called the bone marrow niche.

Hematopoietic stem cell niches are composed of several cell types, including endothelial cells (*6*), osteoblasts (*7–9*), chemokine ligand 12–abundant reticular cells (*10*), nonmyelinating Schwann cells (*11*), and bone marrow mesenchymal stem cells (BM-MSCs) (*12*). These cells appear to control the self-renewal, differentiation, hibernation, and mobilization of hematopoietic stem cells. It is thought that CSCs may form a niche similar to that of hematopoietic stem cells; indeed, some reports have demonstrated the existence of niche-regulating CSCs (*13*, *14*). Furthermore, because BM-MSCs have been found to be associated with breast cancer metastases (*15*), we hypothesized that breast CSCs, similar to hematopoietic stem cells, have a niche composed of BM-MSCs.

Exosomes, which are small intraluminal vesicles of multivesicular bodies released upon exocytic fusion with plasma membranes, are secreted from numerous types of cells and function in intercellular communication by transporting intracellular contents, such as protein, mRNA, and microRNAs (miRNAs) (*16*, *17*). Exosomes secreted by cancer cells may play an important role in cancer progression by promoting angiogenesis (*18*), neutrophil infiltration (*19*), and the education of bone marrow–derived cells (*20*). In turn, exosomes secreted by stromal cells in the tumor microenvironment may contribute to cancer progression through the transmission of their cargo to cancer cells (*21*, *22*). Therefore, we hypothesized that exosomes secreted by BM-MSCs could influence the dormant state of metastatic breast CSCs and investigated the molecular cargo that enabled this switch.

[1]Division of Molecular and Cellular Medicine, National Cancer Center Research Institute, Tokyo 104-0045, Japan. [2]Department of Pathology and Clinical Laboratories, National Cancer Center Hospital, Tokyo 104-0045, Japan. [3]Department of Pathology, National Defense Medical College, Saitama 359-0042, Japan. [4]Breast and Medical Oncology Division, National Cancer Center Hospital, Tokyo 104-0045, Japan.
*Corresponding author. E-mail: tochiya@ncc.go.jp

RESULTS

Establishment of a metastatic breast cancer cell line that exhibits homing to bone marrow

We established a breast cancer cell line that exhibited metastatic homing to bone marrow by injecting C.B-17/Icr-scid/scidJc1 mice with MDA-MB-231 cells expressing luciferase and green fluorescent protein (GFP), monitoring metastasis with bioluminescence, and analyzing the bone marrow for metastatic cells (fig. S1A). The resulting clone from the bone marrow was confirmed to be GFP-positive, indicating that these cells originated from the parental cell line (fig. S1B), and was named MDA-MB-231-BM2 (or BM2, for short). Whereas about half the population of the parental MDA-MB-231-luc-D3H2LN-GFP cells exhibited surface abundance of CD24, the bulk of the BM2 clone did not (fig. S1C), indicating that the bulk of the BM2 clone had a characteristic of breast CSCs. In addition, the expression of many genes was similar in BM2 cells and parental cells; however, the expression of genes related to the cell cycle was decreased in BM2 cells compared with the parental cells (fig. S2, A and B).

Coculture of breast cancer cells with BM-MSCs to induce dormancy

The microenvironment plays an important role in tumor development, progression, and metastatic seeding. To determine the effects of BM-MSCs on BM2 cells, we cocultured BM2 cells with BM-MSCs derived from each of four human donors (table S1). We first confirmed that the BM-MSCs were positive for CD73, CD90, and CD105, surface markers of BM-MSCs (fig. S3). BM2 cells were labeled with the lipophilic dye PKH26, which is retained in dormant or slow-cycling cells in culture (*23*). PKH26-labeled BM2 cells were cocultured with BM-MSCs from different donors at ratio of 1 to 1. As a control, a culture of BM2 cells was incubated alone. We confirmed that almost all of the BM2 cells in either culture were positive for PKH26 on day 0 after labeling (fig. S4). Through microscopic analysis 72 hours later, we observed that BM2 cells cocultured with BM-MSCs retained PKH26 labeling more so than did BM2 cells cultured alone (Fig. 1A). Simultaneously, through flow cytometric analysis, we found that the positive-to-negative ratio of PKH26-labeled cells was greater in BM2 cells cocultured with BM-MSCs compared with those cultured in isolation (Fig. 1B). Additionally, we confirmed a change toward a dormant state in BM2 cells cocultured with BM-MSCs with cell cycle analysis, in which trends for the number of cells in the $G_{2/M}$ phase decreased and the number of cells in the G_0/G_1 phase increased in BM2 cells cocultured with BM-MSC compared with BM2 cells cultured alone (Fig. 1C). These findings indicated that a proportion of BM2 cells acquired dormancy after coculture with BM-MSCs.

From among several BM-MSC cultures, we selected a relatively potent line, R14. Using the R14 cell line, we examined the surface abundance of CD44 and CD24 on cocultured BM2 cells to investigate whether CSC characteristics were changed by coculture with BM-MSCs. We found that the number of CD44-negative ($CD44^-$) cells in cocultures markedly increased compared with that in lone BM2 cultures (Fig. 1D), although CD24 surface abundance was not different between the two (Fig. 1E). In addition, $CD44^-$ cells sorted from the cocultured BM2 cells became $CD44^+$ after several weeks of monoculture (Fig. 1F). These findings show that CD44 abundance as a CSC marker on BM2 cells was decreased by coculture with BM-MSCs, suggesting that cell proliferation and migration of BM2 cells might be affected as well as the change of surface abundance of CSC marker.

Different properties of $CD44^-$ cells and $CD44^+$ cells

To investigate whether decreased surface abundance of CD44 after coculture with BM-MSCs was correlated with the finding that the BM2 cell

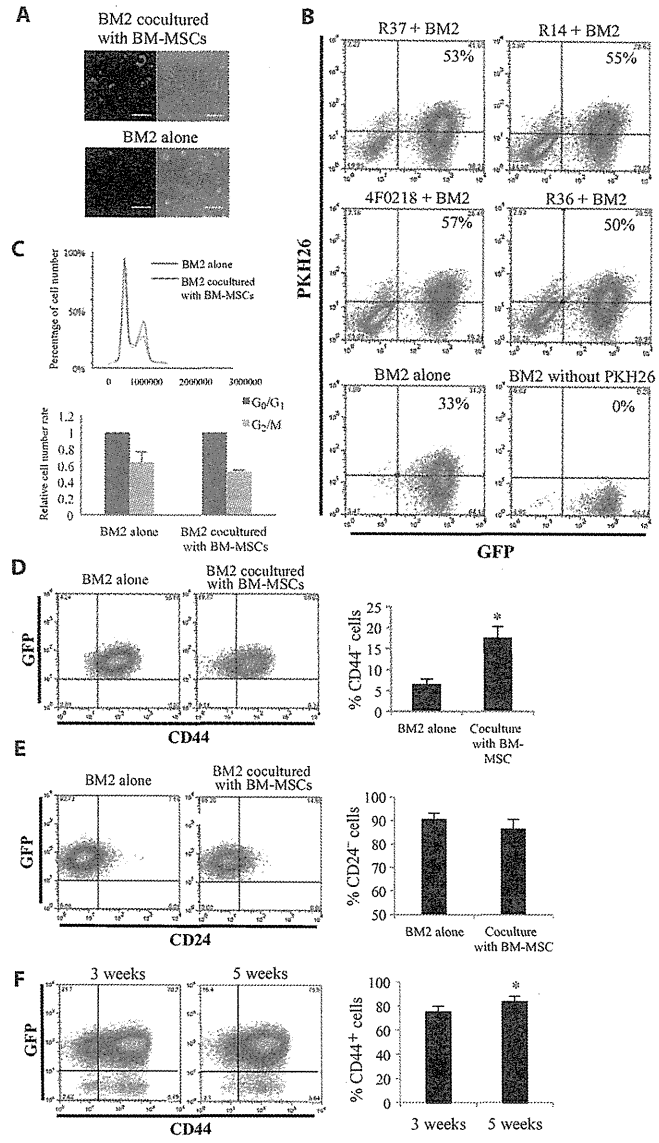

Fig. 1. Acquisition of dormancy in breast CSCs cocultured with BM-MSCs. (A and B) Microscopy (A) and flow cytometry (B) for PKH26 retention in PKH26-labeled BM2 cells cocultured with BM-MSCs for 72 hours compared with BM2 cells cultured alone. Scale bars, 100 μm. Data are representative of three experiments. (C) Cell cycle analyses using Hoechst 33342 in BM2 cells cultured alone or cocultured with R14 BM-MSCs. Data are means ± SE (n = 3; P = 0.20, Student's t test). (D) Flow cytometric analyses of CD44 abundance in BM2 cells cultured alone or cocultured with R14 BM-MSCs (upper panel). Data are means ± SE of three experiments; $^*P < 0.05$, Student's t test. (E) Flow cytometric analyses of CD24 abundance in BM2 cells cultured alone or cocultured with R14 BM-MSCs. (F) $CD44^-$ cells were sorted from BM2 and R14 BM-MSC coculture and BM2 cells cultured alone for up to 5 weeks; flow cytometric analysis of CD44 abundance was performed at 3 or 5 weeks. Data in (E) and (F) are means ± SE of three experiments; (E) P = 0.10, (F) $^*P < 0.05$, Student's t test.

line acquired dormancy, we compared the characteristics of $CD44^-$ cells and $CD44^+$ cells. We sorted BM2 cells cocultured with BM-MSCs into $CD44^-$ and $CD44^+$ populations and confirmed the *CD44* expression status in each using immunocytochemistry and quantitative real-time polymerase chain reaction (qRT-PCR) (fig. S5, A and B). We then examined each population for proliferation, invasive capacity, and drug sensitivity. $CD44^-$ cells had significantly decreased proliferation (Fig. 2A) and a significantly decreased invasion capacity compared with $CD44^+$ cells (Fig. 2B). Furthermore, $CD44^-$ cells were less sensitive to docetaxel, a common breast cancer therapeutic, than $CD44^+$ cells (Fig. 2C). Finally, we confirmed that the global gene expression patterns of the $CD44^+$ and $CD44^-$ BM2 cells were similar, although some genes that encode proteins that influence breast cancer cell dormancy, such as *SRC* (*24*) and *ERBB2* (*25*), were increased and decreased, respectively, in the $CD44^-$ population (fig. S6, A and B). These findings provided evidence that the increased proportion of $CD44^-$ cells in BM2 cultures induced by BM-MSCs was associated with the acquisition of dormancy.

Contribution of BM-MSC–derived exosomes to the acquisition of dormancy in BM2 cells

Next, we investigated how BM-MSCs promoted a dormant phenotype in BM2 cell cultures. We found that culturing BM2 cells in a BM-MSC–conditioned medium increased the number of $CD44^-$ BM2 cells (Fig. 3A), suggesting that a factor secreted by BM-MSCs was responsible for the dormant state of BM2 cells. Therefore, we investigated the role of exosomes derived from BM-MSCs in the dormancy of BM2 cells. We isolated exosomes from R14 BM-MSC–conditioned medium using standard ultracentrifugation. Using phase-contrast electron microscopy and nanoparticle tracking analysis (NTA), we determined that BM-MSC–derived exosomes were about 100 to 200 nm in width, similar to the size of extracellular vesicles (fig. S7A), and physically homogeneous, with most exosomes exhibiting a size of 120 to 160 nm (fig. S7B). Through immunoblotting, we confirmed that the exosomes were positive for the known exosome markers CD9 and CD81 (fig. S7C). Furthermore, using SYTO64 dye, we detected the migration of secreted nucleic acids from BM-MSCs into cocultured BM2 cells (Fig. 3B and fig. S8), and PKH26-labeled exosomes derived from BM-MSCs were taken up by BM2 cells (Fig. 3C and fig. S9). To test whether BM-MSC–derived exosomes could induce dormancy in BM2 cells, we treated PKH26-labeled BM2 cells with exosomes derived from BM-MSCs. After 3 days of incubation, we performed flow cytometry and found that the exosome treatment maintained higher levels of PKH26 abundance on BM2 cells, meaning induction of dormancy in a portion of BM2 cells treated with BM-MSC–derived exosome (Fig. 3D and fig. S10A). In addition, CD44 surface abundance was decreased in BM2 cells treated with BM-MSC–derived exosomes (Fig. 3E and fig. S10B).

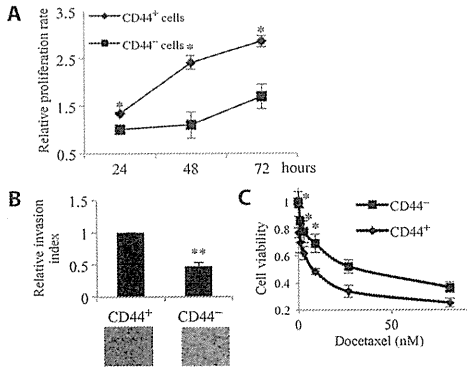

Fig. 2. Phenotypic differences between $CD44^+$ and $CD44^-$ cells. The characteristics of $CD44^+$ and $CD44^-$ cells sorted from BM2 cells by flow cytometry were compared. (A) Cell proliferation normalized to that in $CD44^-$ cells at 24 hours. Each bar represents the mean ± SE ($n = 3$; $^*P < 0.05$). (B) Cell invasion by $CD44^+$ and $CD44^-$ cells normalized to that in $CD44^+$ cells. Data are means ± SE ($n = 3$; $^{**}P < 0.001$ versus $CD44^+$ cells, Student's *t* test). Scale bar, 100 μm. (C) Cell proliferation after docetaxel treatment ($n = 3$; $^*P < 0.05$, Student's *t* test).

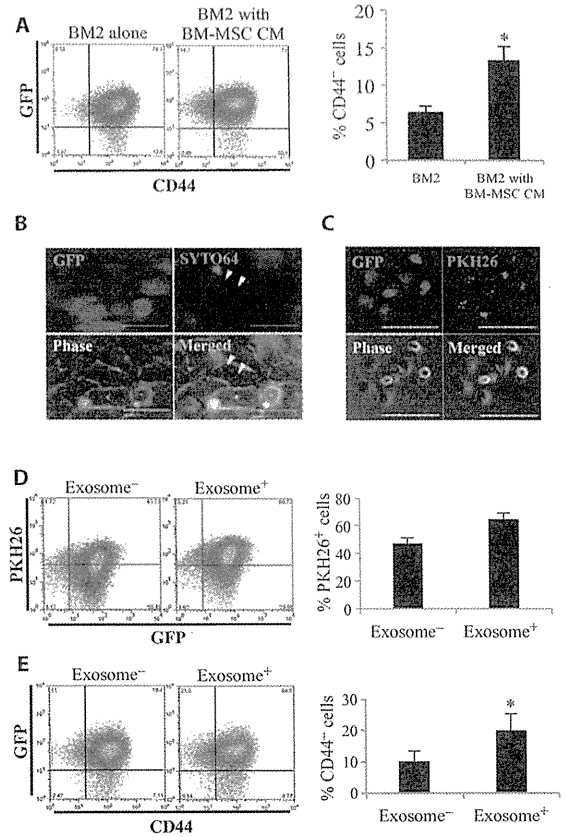

Fig. 3. Induction of a dormant state in BM2 cells by BM-MSC–derived exosomes. (A) Flow cytometric analysis of CD44 abundance in BM2 cells cultured with conditioned medium (CM) derived from R14 BM-MSCs. Each bar represents the mean ± SE ($n = 3$; $^*P < 0.05$, Student's *t* test). (B) BM2 cells were cocultured with SYTO64-labeled R14 BM-MSCs, and images were obtained after 24 hours of coculture. Scale bars, 50 μm. The migration of secreted nucleic acids from BM-MSCs into cocultured BM2 cells was detected (white arrow). (C) PKH26-labeled exosomes derived from R14 BM-MSCs were added to BM2 cells. After incubation for 24 hours, images were obtained. Scale bars, 100 μm. (D) PKH26-labeled BM2 cells were treated with exosomes derived from R14 BM-MSCs or phosphate-buffered saline (PBS). After incubation for 72 hours, PKH26 abundance was analyzed by flow cytometry. Data are means ± SE ($n = 3$; $P = 0.07$, Student's *t* test). (E) R14 BM-MSC–derived exosomes or PBS was added to BM2 cells. After incubation for 1 week, flow cytometry was performed to assess CD44 abundance. Data are means ± SE ($n = 3$; $^*P < 0.05$, Student's *t* test).

Common characteristics between BM2 cells treated with BM-MSC–derived exosomes and CD44⁻ BM2 cells

To investigate the characteristics exhibited by BM2 cells treated with BM-MSC–derived exosomes, we treated the $CD44^+$ fraction of BM2 cells with BM-MSC–derived exosomes or PBS as a control and performed several experiments. First, we examined cell proliferation in $CD44^+$ BM2 cells treated with or without BM-MSC–derived exosomes and found that the $CD44^+$ cells treated with exosomes had significantly decreased cell proliferation (Fig. 4A and fig. S11A) and cell invasion (Fig. 4B and fig. S11B) compared with those cultured alone, although invasion exhibited by cells cultured with R37-dervied exosomes was not significantly decreased. These findings were validated using exosomes derived from BM-MSCs isolated from other volunteers (fig. S11, A and B). To confirm that BM-MSC–derived exosomes could also affect the characteristics of BM2 cells in vivo, BM-MSC–derived exosomes or the same volume of PBS was added to cultures of BM2 cells at days 1 and 4 and incubated for 7 days before being injected into the mammary fat pads of severe combined immunodeficient (SCID) mice. Twenty days after injection, the luciferase activity in tumors resulting from BM2 cell proliferation was lower in the mice implanted with BM-MSC–derived exosome-treated cells than that in controls (Fig. 4C), indicating that the exosomes slowed tumor growth (or tumor formation) by BM2 cells. Additionally, exosome-treated $CD44^+$ BM2 cells exhibited somewhat greater drug resistance compared with cultures lacking exosomes (Fig. 4D and fig. S11C), although the effect of R37-derived exosomes was not statistically significant. These findings suggested that the characteristics of the exosome-treated $CD44^+$ cells were shared by the $CD44^-$ cells in dormant BM2 cells by decreasing surface abundance of CD44 in BM2 cell population.

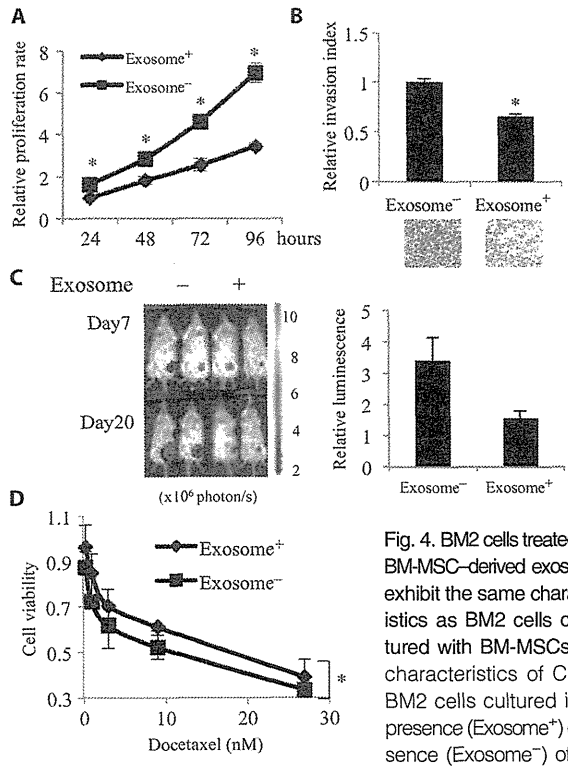

Fig. 4. BM2 cells treated with BM-MSC–derived exosomes exhibit the same characteristics as BM2 cells cocultured with BM-MSCs. The characteristics of $CD44^+$ BM2 cells cultured in the presence ($Exosome^+$) or absence ($Exosome^-$) of R14 BM-MSC–derived exosomes were compared. BM2 cells not cocultured with exosomes were treated with PBS. (A) Cell proliferation in $CD44^+$ BM2 cells cultured with exosomes normalized to that in cells cultured in the absence of exosomes at 24 hours. Data are means ± SE ($n = 3$; $^*P < 0.01$, Student's t test). (B) Cell invasion by $CD44^+$ BM2 cells cultured with or without exosomes, normalized to the invasion index of cells cultured without exosomes. Data are means ± SE ($n = 3$; $^*P < 0.05$ versus cells without exosomes, Student's t test). Scale bar, 100 μm. (C) Bioluminescence quantification in an orthotopic xenograft mouse model of tumors derived from $CD44^+$ BM2 cells cultured in the presence or absence of exosomes. Data are means ± SE ($n = 5$ mice; $P = 0.42$, Student's t test) compared with $CD44^+$ BM2 cells treated without exosomes at day 20. (D) Proliferation of $CD44^+$ BM2 cells treated with docetaxel alone or in the presence of exosomes ($n = 3$; $^*P < 0.01$, Student's t test).

Dormancy in BM2 cultures from exosomal miRNAs derived from BM-MSCs

We next explored which aspects of BM-MSC–derived exosomes promoted dormancy in BM2 cells. Because exosomes contain a large number of miRNAs that diversely influence on cells, we hypothesized that miRNAs in the BM-MSC–derived exosomes contributed to the dormant state of BM2 cells through exosome-mediated transfer. We analyzed the miRNA abundance signature in BM-MSC–derived exosomes compared with that in adult fibroblasts as a control and identified 44 miRNAs with a more than twofold increase in expression in R14 BM-MSC–derived exosomes (table S2). Of these, we selected miR-23b on the basis of previous reports showing that miR-23b suppresses cell invasion and migration or that it contributes to cell cycle arrest and the inhibition of cell proliferation (*26*, *27*). Using qRT-PCR, we confirmed that the abundance of *miR-23b* was more than twofold greater in R14 BM-MSC–derived exosomes compared with that in the adult fibroblasts (fig. S12).

To investigate whether miR-23b affected the dormant state of BM2 cells, PKH26-labeled BM2 cells were transfected with ectopic miR-23b or an empty expression vector as a negative control. Overexpression of miR-23b was confirmed by qRT-PCR (fig. S13). Three days after transfection, we found that BM2 cells transfected with miR-23b had a somewhat greater proportion of PKH26-positive cells than those transfected with the control (Fig. 5A). In addition, we investigated whether the overexpression of miR-23b modulated the surface abundance of CD44 in BM2 cell cultures. $CD44^+$ BM2 cells were transfected with miR-23b or the negative control vector. We found that the $CD44^-$ proportion of the cell population increased by 10% upon overexpression of miR-23b (Fig. 5B). These findings indicated that exosomal miR-23b was responsible for the induction of dormancy in BM2 cells. We also found that the $CD44^+$ BM2 cells with miR-23b overexpression had decreased cell proliferation (fig. S14A) and relatively decreased cell invasion compared with the control, although the latter was not statistically significant (fig. S14B). Additionally, we performed an orthotopic injection of miR-23b–transfected BM2 cells into the mammary fat pads of SCID mice. Twelve days later, we found that the luciferase activity in tumors resulting from miR-23b–transfected BM2 cells was somewhat, but not significantly, decreased compared with that in tumors from control cells (Fig. 5C), indicating that miR-23b may decrease cell proliferation in vivo. Together, these results suggested that bone marrow–secreted miR-23b may contribute to the induction of dormancy in disseminated breast cancer cells.

Targets of exosomal miR-23b in BM2 cells

To identify the target of miR-23b that mediated dormancy induction in BM2 cells, we used in silico information (TargetScan and miRanda) to determine that miR-23b targets genes and identified several cell cycle–related genes, including *CCNG1*, *CDC40*, *CDC23*, *CDC6*, *E2F6*, *HDAC7*, and

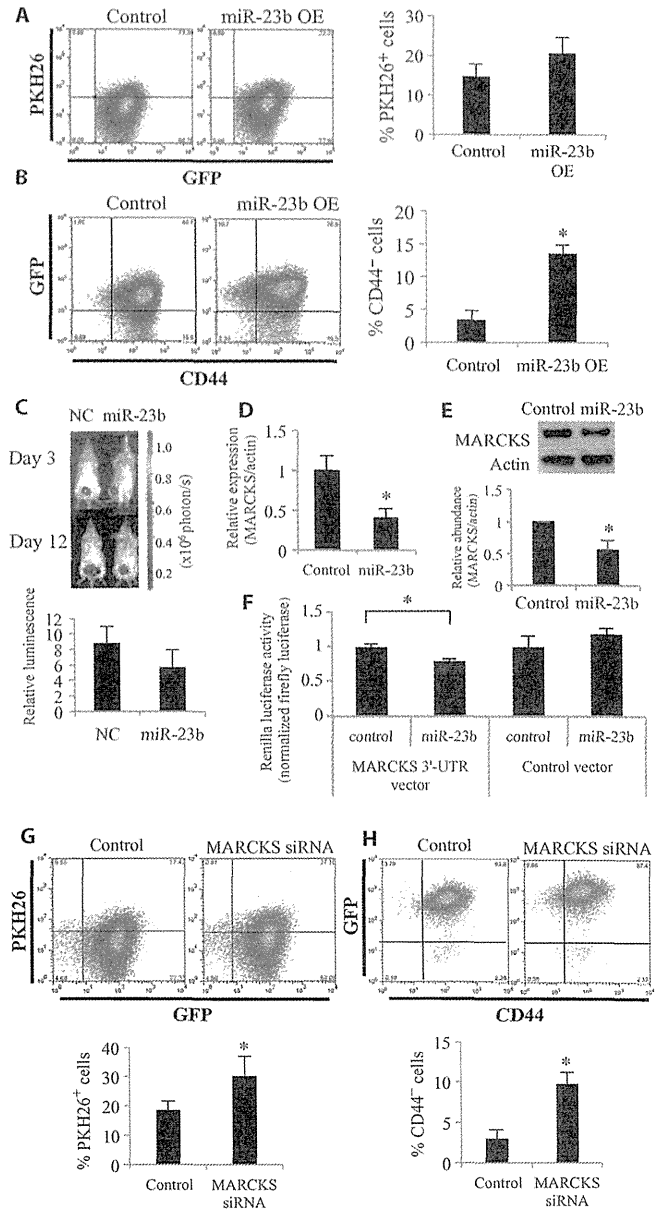

Fig. 5. Suppression of *MARCKS* by miR-23b. (A) Flow cytometric analysis of the PKH26 retention in PKH26-labeled BM2 cells transfected with miR-23b (miR-23b OE) or a negative control vector (control). Data are means ± SE ($n = 3$; $P = 0.08$, Student's t test). (B) Flow cytometric analysis of CD44 abundance in $CD44^+$ BM2 cells transfected with miR-23b (miR-23b OE) or negative control (control). Data are means ± SE ($n = 3$; $^*P < 0.05$, Student's t test). (C) Bioluminescence quantification in an orthotopic xenograft mouse model of tumors derived from miR-23b–overexpressing BM2 cells (miR-23b) ($n = 5$ tumors) or negative control–transfected cells (NC) ($n = 4$ tumors). Data are means ± SE ($P = 0.60$, Student's t test). (D) Expression of *MARCKS* in BM2 cells transfected with miR-23b or a negative control vector (control) was analyzed by qRT-PCR. Data are means ± SE ($n = 3$; $^*P < 0.05$, Student's t test). (E) Immunoblot analysis of MARCKS against β-actin derived from BM2 cells transfected with miR-23b or control vector. Equal amounts of protein concentration were analyzed by immunoblotting. Data are means ± SE ($n = 3$; $P = 0.04$, Student's t test). (F) 3′UTR reporter assay using HEK293 cells. HEK293 cells were cotransfected with hsa-miR-23b or negative control (control) and MARCKS 3′UTR vector or with its control vector. After 48 hours, luciferase activity was measured ($n = 8$; $^*P < 0.004$, Student's t test). (G and H) PKH26-labeled BM2 cells were transfected with MARCKS siRNA or a control siRNA (control). PKH26 retention (G) and CD44 abundance (H) were analyzed by flow cytometry 72 hours later. Data are means ± SE ($n = 3$; $^*P < 0.05$, Student's t test).

YWHAG (table S3). In particular, miR-23b targeted *MARCKS*, which encodes myristoylated alanine-rich C kinase substrate. MARCKS promotes cell motility and cycling and is implicated in the pathogenesis of metastatic cancers (*28*). Using qRT-PCR, we found that *MARCKS* expression in BM2 cells transfected with miR-23b was significantly decreased compared with cells transfected with a negative control (Fig. 5D). In addition, we confirmed that the abundance of MARCKS was decreased in miR-23b–transfected BM2 cells compared with controls (Fig. 5E), and that miR-23b bound directly to the 3′ untranslated region (3′UTR) of *MARCKS* and suppressed its transcription in human embryonic kidney (HEK) 293 cells (Fig. 5F). Furthermore, we analyzed the expression of *miR-23b* in BM2 cells treated with BM-MSC–derived exosomes and found that the expression of *miR-23b* was significantly increased and *MARCKS* expression significantly decreased in BM2 cells treated with exosomes compared with untreated cells (fig. S15). Finally, we performed a flow cytometric analysis of BM2 cells transfected with a small interfering RNA (siRNA) against *MARCKS* or a negative control siRNA. We found that the MARCKS knockdown in BM2 cells (fig. S16) induced dormancy as inferred from an increase in the proportion of PKH26-positive BM2 cells and decreased the surface abundance of CD44 compared with those transfected with the control (Fig. 5, G and H). Additionally, $CD44^+$ BM2 cells transfected with MARCKS siRNA had decreased cell proliferation and invasion (fig. S17, A and B) compared with those transfected with the control. Together, these findings demonstrated that exosomal transfer of miR-23b from BM-MSCs decreased *MARCKS* expression in BM2 cells, promoting the acquisition of dormancy.

BM-MSCs adjacent to breast cancer cells in the bone marrow of breast cancer patients

To corroborate our findings in humans, we examined clinical samples from breast cancer patients in whom cancer cells had metastasized to bone marrow. We performed immunohistochemical analysis of bone marrow specimens from three patients with breast cancer metastases to bone marrow to examine the relationship between breast cancer cells and BM-MSCs. In the bone marrow, BM-MSCs were observed among or adjacent to clusters of breast cancer cells (Fig. 6A), confirming that BM-MSCs coexisted with breast cancer cells in bone marrow in breast cancer patients. Using laser capture microdissection, we isolated cancer cells from both bone marrow and primary breast tissue from 10 patients who presented with breast cancer metastasis to the bone marrow. We found that the expression of *miR-23b* trended higher and that of *MARCKS* trended lower in the cancer cells isolated from bone marrow compared with those from primary breast tissue (Fig. 6B), although neither was statistically significant. The patient data generally support our findings in cells and mice, and suggest that this mechanism may contribute to the dormant phenotype of disseminated breast cancer cells in the bone marrow.

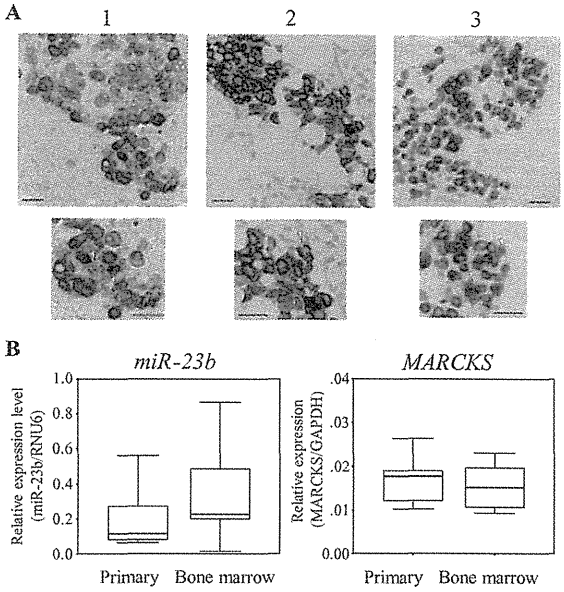

Fig. 6. Analysis of clinical samples from patients with breast cancer metastasis to bone marrow. (A) Immunohistochemical analyses of bone marrow from three patients (numbered 1, 2, and 3) with breast cancer that metastasized to bone marrow were performed. CD105 (brown) and cytokeratin (purple) stainings indicate BM-MSCs and breast cancer cells, respectively. (B) miR-23b and *MARCKS* expression in breast cancer cells in primary lesions and in bone marrow (n = 10; miR-23b, P = 0.13; *MARCKS*, P = 0.87; Wilcoxon test).

DISCUSSION

The microenvironment contains many factors and cell types, such as immune cells, stromal cells, and endothelial cells, that influence cancer progression (*29*). Cancer cells and surrounding noncancerous cells interact by secreting exosomes. It has been demonstrated that exosomes derived from noncancerous cells influence cancer progression and metastasis. Fibroblast-secreted exosomes promote breast cancer cell migration by activating autocrine Wnt–PCP (planar cell polarity) signaling in breast cancer cells (*21*), and BM-MSC–derived exosomes facilitate the progression of multiple myelomas through the transfer of miR-15a (*22*). Moreover, several studies have reported that cancer cell–derived exosomes contribute to cancer progression by inducing changes in surrounding noncancerous cells. For example, melanoma-secreted exosomes enable bone marrow progenitor cells to travel to secondary organs (*20*), and Kosaka *et al.* (*18*) showed that exosomes secreted from breast cancer cells drove endothelial cells to promote angiogenesis, enabling cancer metastasis. Furthermore, neutrophil infiltration, which promotes tumor formation and metastasis, was found to be promoted by cancer cell–derived exosomes (*19*). Thus, there are increasing reports about the role of exosomes in cancer biology. Here, we demonstrated that BM-MSCs play an important role in inducing dormancy in $CD44^+/CD24^-$ breast CSCs in bone marrow through the transfer of a cell cycle inhibitory miRNA, indicating that breast CSCs are maintained by surrounding noncancerous BM-MSCs.

Some reports indicated that a vascular niche composed of endothelial cells maintains CSC "stemness" in skin tumors (*13*) and brain tumors (*14*). Ghajar *et al.* (*30*) also determined that a stable microvasculature formed a niche for cancer cell dormancy, although they did not refer to CSCs. These findings suggested that CSCs are maintained by a microenvironment similar to those of normal stem cells, such as hematopoietic stem cells and neural stem cells (*6*, *31*). Here, we identified BM-MSCs, which constitute niche-regulating hematopoietic stem cells, promote breast CSC dormancy. Although it is believed that bone marrow functions as a reservoir for disseminated tumor cells and that metastasis to secondary organs occurs because of the recirculation of disseminated tumor cells from bone marrow, the precise mechanisms remain unclear. It was reported that periostin, a component of the extracellular matrix derived from stromal cells, was required for the colonization of breast CSCs after their metastasis to secondary organs (*32*). Our study demonstrated mechanisms of maintaining breast CSCs in a dormant state in bone marrow that may occur before their metastatic growth there or in target organs. In addition, we found that the surface abundance of CD44, a characteristic marker of breast CSCs, was decreased in BM2 cultures that acquired dormant phenotypes. It is reported that $CD44^+/CD24^-$ cells are breast CSCs, defined largely by their tumorigenicity in mouse studies. However, although tumorigenicity is considered a feature of CSCs (*33*), it does not indicate dormancy in stem cells. It is possible that changes in CD44 surface abundance are reversible and that cells regain tumorigenicity with time or in response to conditions in the microenvironment.

In addition, we discovered that the effects of BM-MSCs on breast CSCs were attributable to the transfer of miRNAs from BM-MSCs to breast CSCs through exosomes. We revealed that exosomal miR-23b promoted dormancy and decreased CD44 surface abundance in breast cancer cells. In agreement with our study, miR-23b induces cell cycle arrest in glioma CSCs and suppresses glioma cell migration and invasion (*26*, *27*). We identified *MARCKS* as a target gene of miR-23b through in silico analysis. *MARCKS* expression is associated with the pathogenesis of metastatic cancers, and the inhibition of *MARCKS* expression reduces cell invasion and induces cell cycle arrest in colon cancer (*28*). Using qRT-PCR and immunoblotting, we confirmed that the *MARCKS* expression in BM2 cells transfected with miR-23b was significantly decreased compared with the control. Exosomal miR-23b was transferred to BM2 cells, where it suppressed the *MARCKS* expression. However, in our study, whereas xenografts derived from exosome-treated BM2 cells exhibited substantially decreased tumor growth, xenografts derived from BM2 cells overexpressing miR-23b did not exhibit the same degree of proliferative inhibition, suggesting that factors additional to miR-23b contribute to this effect. Therefore, we conclude that exosomal transfer of miR-23b and its suppression of *MARCKS* is one of the mechanisms contributing to cell cycle suppression and dormancy in breast CSCs.

Here, we focused on how cancer cells maintain a dormant state before cancer recurrence, and our findings provide new insights into that issue. From this viewpoint, it is feasible that the mechanism by which cancer cells switch from a dormant state to a proliferative state should function when cancer recurs; however, we did not address this point in this study. Further research is needed to clarify that mechanism. Because exosomes include not only miRNAs but also many types of mRNAs, proteins, and cytokines (*16*, *17*), it is possible that certain proteins function additively. In addition, in this study, the induction of dormancy occurred in only about 10% of cancer cells, suggesting that although miR-23b–mediated suppression of *MARCKS* contributes, there are likely multiple mechanisms that cooperate to promote dormancy in breast CSCs. Nonetheless, our findings suggest that targeting molecules secreted through exosomes from metastatic niches may prevent or delay cancer recurrence.

MATERIALS AND METHODS

Cell culture and establishment of a bone marrow–metastatic breast cancer cell line

Donor information for the human BM-MSC lines R14, R36, R37 (RIKEN), and 4F0218 (Cambrex) is provided in table S1. BM-MSCs were routinely

cultured in MesenPRO RS medium (Invitrogen) containing 2% serum and supplemented with 2 mM GlutaMAX and an antibiotic-antimycotic [penicillin (100 U/ml), streptomycin (100 μg/ml), and amphotericin B (0.25 μg/ml)] (Invitrogen) at 37°C in 5% CO_2. All BM-MSCs were used by the 10th passage. For the coculture of breast cancer cells with BM-MSCs, equal proportions of BM2 cells and BM-MSCs were cocultured in MesenPRO RS medium as described for BM-MSCs. To obtain BM-MSC–conditioned medium, the medium was collected after 2 to 3 days of incubation with the relevant BM-MSC line and centrifuged at 2000*g* for 10 min at 4°C. Supernatant was filtered through a 0.22-μm filter unit (Millipore) to thoroughly remove the cellular debris. Conditioned medium was then ultracentrifuged at 110,000*g* for 70 min at 4°C. Pellets were washed with 11 ml of PBS, ultracentrifuged again, and resuspended in PBS. The protein content of the exosome fraction was measured using the Micro BCA Protein Assay Kit (Thermo Scientific). To track metastasis and establish a bone marrow–metastatic cell line, lentiviral infection of MDA-MB-231-luc-D3H2LN cells (Xenogen) was performed with the pGreenPuro Scramble Hairpin Control (construct MZIP000-PA-1, System Biosciences) to establish breast cancer cells that stably expressed both firefly luciferase and a GFP cloned from copepod *Pontellina plumata* (cop-GFP, also known as ppluGFP2). These cells, which we called MDA-MB-231-luc-D3H2LN-GFP, were cultured in RPMI 1640 containing 10% heat-inactivated fetal bovine serum (FBS) and the antibiotic-antimycotic (above) at 37°C in 5% CO_2. The left heart ventricle of 8-week-old female C.B-17/Icr-scid/scidJc1 mice (Crea Japan) was injected with 1×10^5 MDA-MB-231-luc-D3H2LN-GFP cells suspended in 100 μl of PBS. The subsequent development of metastasis was monitored by injecting luciferin into the mice and measuring bioluminescence using an IVIS imaging system and Living Image 2.50 analysis software (Xenogen). On day 10, bioluminescence was detected in the bilateral legs of a mouse that had received an intracardiac injection. The mouse was sacrificed, and bone marrow was extracted from the legs, cultured in RPMI 1640 as described for the parental MDA-MB-231-luc-D3H2LN-GFP cell line above, and microscopically analyzed for GFP-positive cells. An MDA-MB-231-luc-D3H2LN-GFP cell was cultured under Zeocin selection to establish clones, which we called BM2 cells, cultured in RPMI 1640 as described above for the parental line.

Patient samples

Human bone marrow tissue samples were derived from breast cancer patients treated at the National Cancer Center Hospital. Samples were fixed in formalin, embedded in paraffin, and sectioned for use in microscopic analysis and laser capture microdissection. This study was approved by the Institutional Review Board.

Cell proliferation assay

Cells (3000) were seeded into each well of a 96-well plate and either untreated or treated as indicated in the figures. To assess the effects of exosomal transfer on docetaxel sensitivity, cells were treated with docetaxel for 2 days. Cell viability as a measure of relative proliferation in an MTS [3-(4,5-dimethylthiazol-2-yl)-5-(3-carboxymethoxyphenyl)-2-(4-sulfophenyl)-2-(4-sulfophenyl)-2*H*-tetrazolium] assay was determined on the indicated days using the Cell Counting Kit-8 (Dojindo) according to the manufacturer's instructions, and the absorbance at 450 nm was measured using an EnVision Multilabel Plate Reader (PerkinElmer, Wallac Oy). $CD44^+$ BM2 cells were used for the exosome experiments, and 1 μg of exosomes or PBS at equal volume was added to each well daily.

Transwell invasion assay

The invasion capacity of BM2 cells was assayed in 24-well BioCoat Matrigel 8-μm invasion chambers according to the manufacturer's protocol (Becton Dickinson). Briefly, 1×10^5 cells in serum-free RPMI 1640 medium were plated in the upper chamber. The bottom chamber contained 10% FBS as a chemoattractant. Noninvasive cells were removed with a cotton swab 22 hours later. The cells that migrated through the membrane and adhered to the lower surface of the membrane were fixed with methanol and stained with Diff-Quick Staining Kit. For quantification, the cells were counted under a microscope in four random fields. All assays were performed in triplicate. The data are presented as the percentage invasion through the Matrigel matrix and membrane relative to the migration through the control membrane. In the examination of exosomes, after $CD44^+$ cells were plated in the upper chamber, 1 μg of exosomes derived from BM-MSCs was added to each chamber.

Cell cycle analyses

BM2 cells and BM-MSCs were either cocultured or cultured separately for 72 hours, then fixed with 4% formaldehyde (Sigma-Aldrich) and washed twice in PBS. The cell nuclei were stained with Hoechst 33342 (1:2000, Invitrogen), and the cells were incubated for 15 min. Images were acquired using a 10× water immersion objective and the nonconfocal ultraviolet channel on an Opera high-content screening system (PerkinElmer).

Cell sorting and flow cytometric analyses

BM2 cells were labeled with a PKH26 Red Fluorescent Labeling Kit (Sigma-Aldrich) according to the manufacturer's protocol and cocultured with BM-MSCs. After 72 hours of coculture, the cells were suspended in their culture medium and subjected to flow cytometric analyses using a JSAN cell sorter (Bay Bioscience). At least 1 million cells were pelleted by centrifugation at 180*g* for 5 min at 4°C. BM2 cells were cocultured with BM-MSCs transfected with miR-23b, treated with BM-MSC–conditioned medium, or 3 μg of exosomes. After 7 days in culture (or 3 days for the transfection of miRNAs), the cells were suspended as described above with 5 μl of a monoclonal mouse antibody against human CD44–allophycocyanin (APC) (clone G44-26, BD Pharmingen) or 10 μl of a monoclonal mouse antibody against human CD24-APC (clone ML5, BioLegend) and incubated for 30 min at 4°C.

Isolation of miRNAs

Total RNA was extracted from cultured cells using the QIAzol reagent and the miRNeasy Mini Kit (Qiagen), and total RNA was extracted from clinical specimens using the RecoverAll Total Nucleic Acid Isolation Kit (Ambion) according to the manufacturer's protocols.

Quantitative real-time polymerase chain reaction

qRT-PCR was performed as previously described (*34*). miRNA expression was quantified using TaqMan miRNA assays (Applied Biosystems). PCR was performed in 96-well plates using the 7300 Real-Time PCR System (Applied Biosystems). All reactions were performed in triplicate. *hRNU6* was used as an invariant control for assessing the expression of cellular miRNAs. The TaqMan probes for *hsa-miR-23b* (*miR-23b*) and *hRNU6* were purchased from Applied Biosystems.

Microarrays

Raw and normalized microarray data are available in the Gene Expression Omnibus (GEO) database (accession numbers GSE57921 and GSE58027). Total RNA was extracted from cultured cells using the QIAzol reagent and the miRNeasy Mini Kit (Qiagen). RNA quantity and quality were determined using a NanoDrop ND-1000 spectrophotometer (Thermo Fisher Scientific Inc.) and an Agilent Bioanalyzer (Agilent Technologies), as recommended. Total RNA was amplified and labeled with cyanine 3 (Cy3) using Low Input Quick Amp Labeling Kit, one-color (Agilent Technologies)

following the manufacturer's instructions. Briefly, 100 ng of total RNA was reversed-transcribed to double-strand complementary DNA (cDNA) using a poly dT-T7 promoter primer. Primer, template RNA, and quality-control transcripts of known concentration and quality were first denatured at 65°C for 10 min and incubated for 2 hours at 40°C with 5× first strand buffer, 0.1 M dithiothreitol, 10 mM deoxynucleotide triphosphate mix, and AffinityScript RNase Block Mix. The AffinityScript enzyme was inactivated at 70°C for 15 min. cDNA products were then used as templates for in vitro transcription to generate fluorescent complementary RNA (cRNA). cDNA products were mixed with a transcription master mix in the presence of T7 RNA polymerase and Cy3-labeled CTP (cytidine 5′-triphosphate) and incubated at 40°C for 2 hours. Labeled cRNA was purified using RNeasy Mini Spin Columns (Qiagen) and eluted in 30 μl of nuclease-free water. After amplification and labeling, cRNA quantity and cyanine incorporation were determined using a NanoDrop ND-1000 spectrophotometer and an Agilent Bioanalyzer. For each hybridization, 0.60 μg of Cy3-labeled cRNA was fragmented and hybridized at 65°C for 17 hours to an Agilent SurePrint G3 Human GE v2 8x60K Microarray (design ID: 039494). After washing, microarrays were scanned using an Agilent DNA microarray scanner. Intensity values of each scanned feature were quantified using Agilent Feature Extraction software version 10.7.3.1, which performs background subtractions. We only used features that were flagged as no errors (present flags) and excluded features that were not positive, not significant, not uniform, not above background, saturated, and population outliers (marginal and absent flags). Normalization was performed with Agilent GeneSpring GX version 12.6.1 (per chip: normalization to 75th percentile shift; per gene: normalization to median of all samples). There are a total of 50,599 probes on Agilent SurePrint G3 Human GE v2 8x60K Microarray (design ID: 039494) without control probes. The altered transcripts were quantified using the comparative method. We applied ≥1.2-fold change in signal intensity to identify the significant differences of gene expression in this study.

Transient miRNA transfection

Synthetic hsa-miR-23b was obtained from Bonac. The AllStars Negative Control siRNA was purchased from Qiagen. The transfection of miRNA and siRNA was accomplished using the DharmaFECT 1 transfection reagent (Thermo Fisher Scientific) according to the manufacturer's protocol. The *hsa-miR-23b* sequences were (5′ to 3′) UGGGUUCCUGGCAUGCUGAUUU (sense) and AUCACAUUGCCAGGGAUUAC (antisense).

Immunohistochemistry

Specimens were formalin-fixed and paraffin-embedded, and 4-μm-thick sections were prepared for immunohistochemistry, performed with antibodies against the BM-MSC marker CD105 (clone SN6, Abcam) and an epithelial marker cytokeratin (clone AE1/AE3, Dako). The sections were deparaffinized and incubated first with the CD105 antibody at room temperature for 1 hour, incubated with a peroxidase-conjugated secondary antibody, and visualized with diaminobenzidine tetrahydrochloride and hydrogen peroxide (CSA II, Dako). Sections were subjected to antigen retrieval by being autoclaved in sodium citrate buffer (pH 6.0) for 10 min at 121°C and allowed to cool to room temperature. Slides were then incubated with a cytokeratin antibody at room temperature for 1 hour, and then incubated with a dextran polymer reagent combined with secondary antibodies and peroxidase (EnVision Plus, Dako) for 2 hours at room temperature. Specific antigen-antibody reactions were visualized using the Vector VIP peroxidase (HRP) Substrate kit.

Immunoblot analysis

Exosomes were lysed in a 2% SDS buffer, and equal amounts of protein were loaded onto an SDS–polyacrylamide gel and transferred onto polyvinylidine difluoride membranes (Bio-Rad Laboratories). Antibodies against CD9 (1:200, Santa Cruz Biotechnology), CD81 (1:200, Santa Cruz Biotechnology), MARCKS (1:5000, Abcam), and β-actin (1:1000, Millipore) were used as primary antibodies. CD9 and CD81 abundance was assessed in nonreducing conditions. As secondary antibodies, HRP (horseradish peroxidase)–linked antibodies against mouse and rabbit immunoglobulin G (GE Healthcare) were used at a dilution of 1:5000. Bound antibodies were visualized by chemiluminescence, and images were analyzed using a LuminoImager (LAS-3000, Fujifilm Inc.).

Nanoparticle tracking analysis

NTA of exosomes resuspended in PBS and further diluted for analysis was performed with the NanoSight LM10-HS system per manufacturer's protocol.

Confocal microscopy

Confocal microscopy was performed with an Olympus FV10i laser scanning microscope. The filters used were 489 to 510 nm (for GFP), 551 to 567 nm (for PKH26), and 599 to 619 nm (for SYTO64).

Phase-contrast transmission electron microscopy

BM-MSC–derived exosomes were visualized using phase-contrast transmission electron microscopy performed by Terabase Inc.

SYTO64-labeled miRNA transfer

BM-MSCs were incubated at 37°C for 7 hours in the presence of 1 μM SYTO64-labeled conditioned medium, the medium was discarded, and the BM-MSCs were washed twice with PBS to remove excess dye. BM2 cells were added to the dish in which BM-MSCs were seeded, and the cells were incubated at 37°C for 24 hours.

PKH26-labeled exosome transfer

Purified exosomes derived from BM-MSCs were labeled with the PKH26 Red Fluorescent Labeling Kit (Sigma). Exosomes were incubated with 2 μM PKH26 for 5 min, washed four times through a 100-kD filter (Microcon YM-100, Millipore) to remove excess dye, and incubated with BM2 cells at 37°C.

Establishment of stable cell lines

Stable BM2 cell lines expressing *miR-23b* were generated by selection with puromycin (2 μg/ml). BM2 cells at 90% confluency were transfected with an hsa-miR-23b expression vector in 24-well dishes using the Lipofectamine LTX Reagent in accordance with the manufacturer's instructions (Life Technologies). Cells were replated in a 10-cm dish 12 hours after transfection, followed by selection with puromycin for 3 weeks. Ten surviving single colonies were picked from each transfectant and cultured for an additional 2 weeks. The cells expressing the largest amount of *miR-23b* among the transfectants were considered to stably express miR-23b.

3′UTR reporter assay plasmid constructs

A 729–base pair fragment from the 3′UTR of *MARCKS*, which contained the predicted target sequences of miR-23b (located at positions 1210 to 1216 and 1654 to 1660 of the *MARCKS* 3′UTR), was cloned by PCR from total RNA isolated from MDA-MB-231 cells. A 3′ polyadenylate overhang was added to the PCR products after 15 min of regular Taq polymerase treatment at 72°C. The PCR products were cloned into a pGEM-T Easy vector (Promega) and ligated into the Not I site of the 3′UTR of the *Rennila* luciferase gene in the psiCHECK-2 plasmid (Promega). The *miR-23b* primer sequences were (5′ to 3′) TGGAGAAGCTTTGACCAATTT (forward) and AAGGCCCATGAACTGACATC (reverse). HEK293 cells were cultured overnight

in 96-well tissue culture plates at densities of 1×10^4 cells per well, respectively, and each construct was cotransfected with hsa-miR-23b using the DharmFECT Duo Transfection Reagent (Thermo Fisher Scientific). The cells were harvested 48 hours after transfection, and the *Rennila* luciferase activity was measured and normalized to the firefly luciferase activity. All assays were performed in triplicate and were repeated at least three times; representative results are shown.

Tumorigenicity assay in SCID mice

BM2 cells (20,000) were seeded into six-well plates, and 3 μg of BM-MSC–derived exosomes or the same amount of PBS was added to each well on days 1 and 4. Five-week-old female C.B-17/Icr-scid/scidJc1 mice (Crea Japan) received mammary fat pad 100-μl injections of PBS containing 1×10^5 BM2 cells that had been cultured with R14 BM-MSC–derived exosomes or PBS for 7 days. Tumor growth was monitored by injecting mice with luciferin and measuring the bioluminescence using an IVIS imaging system (Xenogen). The data were analyzed using Living Image 2.50 software (Xenogen). All experimental protocols involving animals were approved by the Institute for Laboratory Animal Research, National Cancer Center Research Institute.

Statistical analyses

The data presented in bar graphs are means ± SE of at least three independent experiments. The statistical analyses were performed with Student's *t* test or Wilcoxon test. $P < 0.05$ was considered to be statistically significant.

SUPPLEMENTARY MATERIALS

www.sciencesignaling.org/cgi/content/full/7/332/ra63/DC1

Fig. S1. Establishment of a line of breast cancer cells that metastasized to bone marrow.
Fig. S2. Gene expression array in BM2 and parental cells.
Fig. S3. Surface marker profiles of BM-MSCs from human donors.
Fig. S4. Flow cytometric analysis of PKH26 labeling in BM2 cultures.
Fig. S5. CD44 expression and surface abundance on sorted $CD44^+$ and $CD44^-$ cells.
Fig. S6. Gene expression array in $CD44^+$ or $CD44^-$ BM2 cells.
Fig. S7. Characterization of BM-MSC–derived exosomes.
Fig. S8. Images of BM2 cells cocultured with SYTO64-labeled BM-MSCs.
Fig. S9. Images of BM2 cells cocultured with PKH26-labeled exosomes.
Fig. S10. Flow cytometry of BM2 cells cultured with BM-MSC–derived exosomes.
Fig. S11. Proliferation and invasive behavior of BM2 cells cultured with BM-MSC–derived exosomes.
Fig. S12. Expression of *miR-23b* in exosomes derived from BM-MSCs or fibroblasts.
Fig. S13. Overexpression of miR-23b in BM2 cells.
Fig. S14. Proliferation and invasive behavior of BM2 cells overexpressing miR-23b.
Fig. S15. Effect of exosomes on *miR-23b* and *MARCKS* expression in BM2 cells.
Fig. S16. Knockdown of MARCKS in BM2 cells.
Fig. S17. Proliferation and invasive behavior in MARCKS-deficient BM2 cells.
Table S1. Donor information for BM-MSCs.
Table S2. miRNAs that were increased in BM-MSC exosomes.
Table S3. Predicted miR-23b target genes.
Table S4. Expression analysis in BM2 cells.

REFERENCES AND NOTES

1. National Cancer Center for Cancer Control and Information Services, Japan, Cancer mortality (1958–2011). Vital Statistics Japan (Ministry of Health, Labour and Welfare), (2011).
2. J. M. Kurtz, J. M. Spitalier, R. Amalric, Late breast recurrence after lumpectomy and irradiation. *Int. J. Radiat. Oncol. Biol. Phys.* **9**, 1191–1194 (1983).
3. S. Braun, F. D. Vogl, B. Naume, W. Janni, M. P. Osborne, R. C. Coombes, G. Schlimok, I. J. Diel, B. Gerber, G. Gebauer, J. Y. Pierga, C. Marth, D. Oruzio, G. Wiedswang, E. F. Solomayer, G. Kundt, B. Strobl, T. Fehm, G. Y. Wong, J. Bliss, A. Vincent-Salomon, K. Pantel, A pooled analysis of bone marrow micrometastasis in breast cancer. *N. Engl. J. Med.* **353**, 793–802 (2005).
4. M. Balic, H. Lin, L. Young, D. Hawes, A. Giuliano, G. McNamara, R. H. Datar, R. J. Cote, Most early disseminated cancer cells detected in bone marrow of breast cancer patients have a putative breast cancer stem cell phenotype. *Clin. Cancer Res.* **12**, 5615–5621 (2006).
5. K. Pantel, C. Alix-Panabières, S. Riethdorf, Cancer micrometastases. *Nat. Rev. Clin. Oncol.* **6**, 339–351 (2009).
6. M. J. Kiel, O. H. Yilmaz, T. Iwashita, O. H. Yilmaz, C. Terhorst, S. J. Morrison, SLAM family receptors distinguish hematopoietic stem and progenitor cells and reveal endothelial niches for stem cells. *Cell* **121**, 1109–1121 (2005).
7. L. M. Calvi, G. B. Adams, K. W. Weibrecht, J. M. Weber, D. P. Olson, M. C. Knight, R. P. Martin, E. Schipani, P. Divieti, F. R. Bringhurst, L. A. Milner, H. M. Kronenberg, D. T. Scadden, Osteoblastic cells regulate the haematopoietic stem cell niche. *Nature* **425**, 841–846 (2003).
8. F. Arai, A. Hirao, M. Ohmura, H. Sato, S. Matsuoka, K. Takubo, K. Ito, G. Y. Koh, T. Suda, Tie2/Angiopoietin-1 signaling regulates hematopoietic stem cell quiescence in the bone marrow niche. *Cell* **118**, 149–161 (2004).
9. J. Zhang, C. Niu, L. Ye, H. Huang, X. He, W. G. Tong, J. Ross, J. Haug, T. Johnson, J. Q. Feng, S. Harris, L. M. Wiedemann, Y. Mishina, L. Li, Identification of the haematopoietic stem cell niche and control of the niche size. *Nature* **425**, 836–841 (2003).
10. T. Sugiyama, H. Kohara, M. Noda, T. Nagasawa, Maintenance of the hematopoietic stem cell pool by CXCL12-CXCR4 chemokine signaling in bone marrow stromal cell niches. *Immunity* **25**, 977–988 (2006).
11. S. Yamazaki, H. Ema, G. Karlsson, T. Yamaguchi, H. Miyoshi, S. Shioda, M. M. Taketo, S. Karlsson, A. Iwama, H. Nakauchi, Nonmyelinating Schwann cells maintain hematopoietic stem cell hibernation in the bone marrow niche. *Cell* **147**, 1146–1158 (2011).
12. S. Méndez-Ferrer, T. V. Michurina, F. Ferraro, A. R. Mazloom, B. D. Macarthur, S. A. Lira, D. T. Scadden, A. Ma'ayan, G. N. Enikolopov, P. S. Frenette, Mesenchymal and haematopoietic stem cells form a unique bone marrow niche. *Nature* **466**, 829–834 (2010).
13. B. Beck, G. Driessens, S. Goossens, K. K. Youssef, A. Kuchnio, A. Caauwe, P. A. Sotiropoulou, S. Loges, G. Lapouge, A. Candi, G. Mascre, B. Drogat, S. Dekoninck, J. J. Haigh, P. Carmeliet, C. Blanpain, A vascular niche and a VEGF–Nrp1 loop regulate the initiation and stemness of skin tumours. *Nature* **478**, 399–403 (2011).
14. C. Calabrese, H. Poppleton, M. Kocak, T. L. Hogg, C. Fuller, B. Hamner, E. Y. Oh, M. W. Gaber, D. Finklestein, M. Allen, A. Frank, I. T. Bayazitov, S. S. Zakharenko, A. Gajjar, A. Davidoff, R. J. Gilbertson, A perivascular niche for brain tumor stem cells. *Cancer Cell* **11**, 69–82 (2007).
15. A. E. Kamoub, A. B. Dash, A. P. Vo, A. Sullivan, M. W. Brooks, G. W. Bell, A. L. Richardson, K. Polyak, R. Tubo, R. A. Weinberg, Mesenchymal stem cells within tumour stroma promote breast cancer metastasis. *Nature* **449**, 557–563 (2007).
16. H. Valadi, K. Ekström, A. Bossios, M. Sjöstrand, J. J. Lee, J. O. Lötvall, Exosome-mediated transfer of mRNAs and microRNAs is a novel mechanism of genetic exchange between cells. *Nat. Cell Biol.* **9**, 654–659 (2007).
17. J. Skog, T. Würdinger, S. van Rijn, D. H. Meijer, L. Gainche, M. Sena-Esteves, W. T. Curry Jr., B. S. Carter, A. M. Krichevsky, X. O. Breakefield, Glioblastoma microvesicles transport RNA and proteins that promote tumour growth and provide diagnostic biomarkers. *Nat. Cell Biol.* **10**, 1470–1476 (2008).
18. N. Kosaka, H. Iguchi, K. Hagiwara, Y. Yoshioka, F. Takeshita, T. Ochiya, Neutral Sphingomyelinase 2 (nSMase2)-dependent exosomal transfer of angiogenic microRNAs regulate cancer cell metastasis. *J. Biol. Chem.* **288**, 10849–10859 (2013).
19. A. Bobrie, S. Krumeich, F. Reyal, C. Recchi, L. F. Moita, M. C. Seabra, M. Ostrowski, C. Théry, Rab27a supports exosome-dependent and -independent mechanisms that modify the tumor microenvironment and can promote tumor progression. *Cancer Res.* **72**, 4920–4930 (2012).
20. H. Peinado, M. Alečković, S. Lavotshkin, I. Matei, B. Costa-Silva, G. Moreno-Bueno, M. Hergueta-Redondo, C. Williams, G. García-Santos, C. Ghajar, A. Nitadori-Hoshino, C. Hoffman, K. Badal, B. A. Garcia, M. K. Callahan, J. Yuan, V. R. Martins, J. Skog, R. N. Kaplan, M. S. Brady, J. D. Wolchok, P. B. Chapman, Y. Kang, J. Bromberg, D. Lyden, Melanoma exosomes educate bone marrow progenitor cells toward a pro-metastatic phenotype through MET. *Nat. Med.* **18**, 883–891 (2012).
21. V. Luga, L. Zhang, A. M. Viloria-Petit, A. A. Ogunjimi, M. R. Inanlou, E. Chiu, M. Buchanan, A. N. Hosein, M. Basik, J. L. Wrana, Exosomes mediate stromal mobilization of autocrine Wnt-PCP signaling in breast cancer cell migration. *Cell* **151**, 1542–1556 (2012).
22. A. M. Roccaro, A. Sacco, P. Maiso, A. K. Azab, Y. T. Tai, M. Reagan, F. Azab, L. M. Flores, F. Campigotto, E. Weller, K. C. Anderson, D. T. Scadden, I. M. Ghobrial, BM mesenchymal stromal cell-derived exosomes facilitate multiple myeloma progression. *J. Clin. Invest.* **123**, 1542–1555 (2013).
23. S. Pece, D. Tosoni, S. Confalonieri, G. Mazzarol, M. Vecchi, S. Ronzoni, L. Bernard, G. Viale, P. G. Pelicci, P. P. Di Fiore, Biological and molecular heterogeneity of breast cancers correlates with their cancer stem cell content. *Cell* **140**, 62–73 (2010).
24. X. H. Zhang, Q. Wang, W. Gerald, C. A. Hudis, L. Norton, M. Smid, J. A. Foekens, J. Massagué, Latent bone metastasis in breast cancer tied to Src-dependent survival signals. *Cancer Cell* **16**, 67–78 (2009).
25. J. A. Aguirre-Ghiso, Models, mechanisms and clinical evidence for cancer dormancy. *Nat. Rev. Cancer* **7**, 834–846 (2007).
26. J. Geng, H. Luo, Y. Pu, Z. Zhou, X. Wu, W. Xu, Z. Yang, Methylation mediated silencing of miR-23b expression and its role in glioma stem cells. *Neurosci. Lett.* **528**, 185–189 (2012).
27. J. C. Loftus, J. T. Ross, K. M. Paquette, V. M. Paulino, S. Nasser, Z. Yang, J. Kloss, S. Kim, M. E. Berens, N. L. Tran, miRNA expression profiling in migrating glioblastoma

cells: Regulation of cell migration and invasion by miR-23b via targeting of Pyk2. *PLOS One* **7**, e39818 (2012).
28. K. Rombouts, V. Carloni, T. Mello, S. Omenetti, S. Galastri, S. Madiai, A. Galli, M. Pinzani, Myristoylated Alanine-Rich protein Kinase C Substrate (MARCKS) expression modulates the metastatic phenotype in human and murine colon carcinoma in vitro and in vivo. *Cancer Lett.* **333**, 244–252 (2013).
29. J. A. Joyce, J. W. Pollard, Microenvironmental regulation of metastasis. *Nat. Rev. Cancer* **9**, 239–252 (2009).
30. C. M. Ghajar, H. Peinado, H. Mori, I. R. Matei, K. J. Evason, H. Brazier, D. Almeida, A. Koller, K. A. Hajjar, D. Y. Stainier, E. I. Chen, D. Lyden, M. J. Bissell, The perivascular niche regulates breast tumour dormancy. *Nat. Cell Biol.* **15**, 807–817 (2013).
31. A. Louissaint Jr., S. Rao, C. Leventhal, S. A. Goldman, Coordinated interaction of neurogenesis and angiogenesis in the adult songbird brain. *Neuron* **34**, 945–960 (2002).
32. I. Malanchi, A. Santamaria-Martínez, E. Susanto, H. Peng, H. A. Lehr, J. F. Delaloye, J. Huelsken, Interactions between cancer stem cells and their niche govern metastatic colonization. *Nature* **481**, 85–89 (2011).
33. M. Al-Hajj, M. S. Wicha, A. Benito-Hernandez, S. J. Morrison, M. F. Clarke, Prospective identification of tumorigenic breast cancer cells. *Proc. Natl. Acad. Sci. U.S.A.* **100**, 3983–3988 (2003).
34. P. S. Mitchell, R. K. Parkin, E. M. Kroh, B. R. Fritz, S. K. Wyman, E. L. Pogosova-Agadjanyan, A. Peterson, J. Noteboom, K. C. O'Briant, A. Allen, D. W. Lin, N. Urban, C. W. Drescher, B. S. Knudsen, D. L. Stirewalt, R. Gentleman, R. L. Vessella, P. S. Nelson, D. B. Martin, M. Tewari, Circulating microRNAs as stable blood-based markers for cancer detection. *Proc. Natl. Acad. Sci. U.S.A.* **105**, 10513–10518 (2008).

Acknowledgments: We thank N. Kai and I. Konishi (Terabase Inc.) for providing electron microscopy images, and S. Miura, C. Kina, and C. Onuma (National Cancer Center Hospital) and A. Inoue (National Cancer Center Research Institute) for excellent technical support. **Author contributions:** M.O., N.K., and T.O. designed the experiments and wrote the manuscript. M.O., N.K., N.T., Y.Y., F.T., and R.T. performed the experiments. M.Y. and H.T. provided the clinical samples. M.O. and K.T. performed the statistical analysis. **Funding:** This work was supported in part by the Grant-in-Aid for the Third-Term Comprehensive 10-Year Strategy for Cancer Control from the Ministry of Health, Labor, and Welfare, Japan; the Program for Promotion of Fundamental Studies in Health Sciences of the National Institute of Biomedical Innovation; and the Japan Society for the Promotion of Science through the Funding Program for World-Leading Innovative R&D on Science and Technology (FIRST Program) initiated by the Council for Science and Technology Policy. **Competing interests:** The authors declare that they have no competing interests. **Data and materials availability:** The gene expression microarray data are deposited in GEO (http://www.ncbi.nlm.nih.gov/geo/), accession numbers GSE57921 and GSE58027.

Submitted 28 February 2014
Accepted 12 June 2014
Final Publication 1 July 2014
10.1126/scisignal.2005231
Citation: M. Ono, N. Kosaka, N. Tominaga, Y. Yoshioka, F. Takeshita, R.-u Takahashi, M. Yoshida, H. Tsuda, K. Tamura, T. Ochiya, Exosomes from bone marrow mesenchymal stem cells contain a microRNA that promotes dormancy in metastatic breast cancer cells. *Sci. Signal.* **7**, ra63 (2014).

Science Signaling
AAAS

Exosomes from bone marrow mesenchymal stem cells contain a microRNA that promotes dormancy in metastatic breast cancer cells

Makiko Ono, Nobuyoshi Kosaka, Naoomi Tominaga, Yusuke Yoshioka, Fumitaka Takeshita, Ryou-u Takahashi, Masayuki Yoshida, Hitoshi Tsuda, Kenji Tamura and Takahiro Ochiya (July 1, 2014)

Science Signaling 7 (332), ra63. [doi: 10.1126/scisignal.2005231]

Science Signaling (ISSN 1937-9145) is published weekly, except the last December, by the American Association for the Advancement of Science, 1200 New York Avenue, NW, Washington, DC 20005.

Circulating MicroRNAs in Drug Safety Assessment for Hepatic and Cardiovascular Toxicity: The Latest Biomarker Frontier?

Mitsuhiko Osaki, Nobuyoshi Kosaka, Futoshi Okada & Takahiro Ochiya

Molecular Diagnosis & Therapy

ISSN 1177-1062
Volume 18
Number 2

Mol Diagn Ther (2014) 18:121-126
DOI 10.1007/s40291-013-0065-0

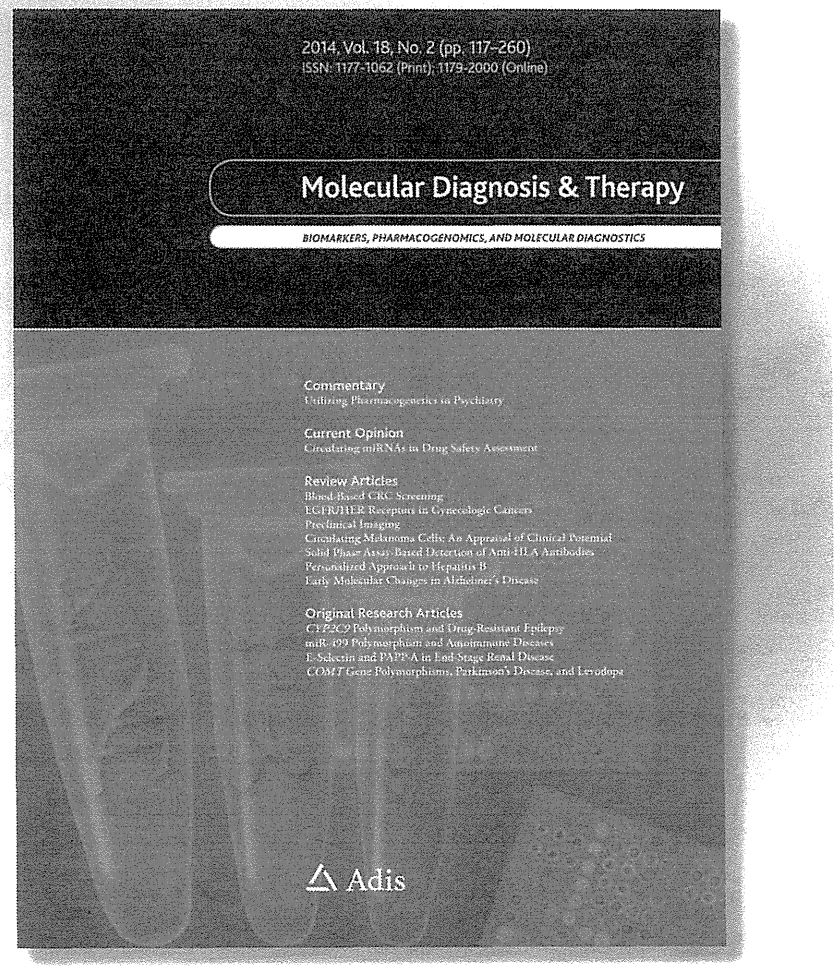

Springer

Mol Diagn Ther (2014) 18:121–126
DOI 10.1007/s40291-013-0065-0

CURRENT OPINION

Circulating MicroRNAs in Drug Safety Assessment for Hepatic and Cardiovascular Toxicity: The Latest Biomarker Frontier?

Mitsuhiko Osaki · Nobuyoshi Kosaka · Futoshi Okada · Takahiro Ochiya

Published online: 6 November 2013

Abstract Drug-induced liver and cardiovascular injuries are important aspects of safety evaluations of numerous drugs in development. Therefore, reliable and predictive biomarkers to allow detection of early signs of drug-induced liver and cardiovascular injuries are required in clinical and preclinical pharmaceutical evaluation. MicroRNAs (miRNAs) are reported to be present in body fluids (blood, urine, etc.), and these 'circulating miRNAs' have been proposed as toxicological biomarkers of drug-induced tissue injury in preclinical and clinical practice. To be used as biomarkers of drug toxicity, such miRNAs need to show rapid and injured-tissue–specific upregulation in body fluids after injury, be more sensitive than existing protein markers such as alanine aminotransferase (ALT) and troponins, and be able to identify the toxicants responsible, if possible. In this article, we focus on the current knowledge of circulating miRNAs, which have potential for use in assessment of drug-induced liver and cardiovascular injuries. In addition, we discuss an important question regarding normalization of the expression levels of certain circulating miRNAs in body fluids.

M. Osaki (✉) · F. Okada
Division of Pathological Biochemistry, Department of Biomedical Sciences, Faculty of Medicine, Tottori University, 86 Nishi-cho, Yonago, Tottori 683-8503, Japan
e-mail: osamitsu@med.tottori-u.ac.jp

M. Osaki · F. Okada
Chromosome Engineering Research Center, Tottori University, 86 Nishi-cho, Yonago, Tottori 683-8503, Japan

N. Kosaka · T. Ochiya
Division of Molecular and Cellular Medicine, National Cancer Center Research Institute, 5-1-1 Tsukiji, Chuo-ku, Tokyo, 104-0045 Japan

1 Introduction

MicroRNAs (miRNAs) are endogenous non-coding RNAs of ~22 bp in length, which suppress gene expression in a sequence-specific manner and play important roles in a wide range of physiological and pathological processes [1, 2]. miRNA was first identified in *Caenorhabditis elegans* as RNA molecules that were complementary to the 3′ untranslated regions of the target transcript, such as the lin-4 and let-7 genes [3, 4]. On the basis of miRBase release 20.0, more than 1,800 human miRNAs have been registered [5], with a large number being evolutionarily conserved [6, 7]. It has been reported that miRNAs are expressed in all animal cells and have fundamental roles in cellular activities such as development, cellular differentiation, proliferation, cell-cycle control, apoptosis, metabolism, and cancer [7]. miRNAs can downregulate gene expression by affecting mRNA stability and influencing protein synthesis in a sequence-specific manner [8]. Similarly to mRNA, some miRNAs are produced in a cell- or tissue-specific manner [9, 10]. Those specific miRNAs would be released to ouside of these cells followed by cell injury. Thus, it is strongly suggested that injured cells or tissues could be identified by detecting such miRNAs circulating in body fluids.

Recent studies have suggested that miRNAs are not only localized within the cell (cellular miRNA) but are also present in extracellular spaces such as body fluids [11–16]. Interestingly, these circulating miRNAs are resistant against RNase- and repetitive freezing and thawing cycle-mediated degradation, owing to the formation of complexes with high-density lipoproteins [17] or Argonaute 2 [18], or envelopment in microvesicles [19, 20], exosomes [21, 22], or apoptotic bodies [23, 24]. miRNAs are detectable and highly stable in circulation [25, 26], making

them attractive for biomarker discovery. On the basis of these findings, the profile of circulating miRNAs in a wide range of body fluids, including urine, blood, cerebrospinal fluid, bronchial lavage, and breast milk, has been exploited as a biomarker in various diseases, including cancer [27], drug-induced tissue injury [9], and inflammation [28]. In oncology, many studies have demonstrated that circulating miRNAs are a potential diagnostic biomarker of chronic lymphocytic leukemia [29], non-small-cell lung cancer [30], colorectal cancer [31], and many other cancers [12, 32]. These data consistently show that circulating miRNAs are potentially useful biomarkers for cancer diagnosis and prognosis. Recently, several studies have reported that the levels of specific circulating miRNAs have been used to detect and monitor tissue injury induced by drugs, although the number of such studies is relatively small.

In this article, we discuss recent findings regarding the potential of circulating miRNAs as biomarkers of liver and cardiovascular toxicity.

2 Use of Circulating miRNAs as Biomarkers of Liver Injury

Drug-induced liver injury is an adverse event that frequently leads to cessation of drug testing in clinical trials, restrictions on drug use, and removal of drugs from the market [33–35]. Assessment of liver injury induced by drugs is a major safety issue during drug development. Existing biomarkers of liver injury—for example, serum alanine aminotransferase (ALT), aspartate aminotransferase (AST), and bilirubin—provide reasonable indicators of damage or altered function [36]; however, serum ALT and AST activities are known to be increased in other organ injuries [37, 38]. A number of exploratory biomarkers are currently under investigation, including high-mobility group box 1, cytokeratin 18, glutamate dehydrogenase, sorbitol dehydrogenase, albumin mRNA, α-glutathione S-transferase, and F-protein [39, 40]. Although several of these exhibit a high degree of sensitivity for early liver injury and varying degrees of cell-type specificity, they do not discriminate between drug and non-drug etiologies. Therefore, reliable new biomarkers of liver injury are urgently required for clinical use and for preclinical pharmaceutical evaluation. In recent years, several studies have demonstrated the possibility of evaluating drug-induced liver injury by measuring circulating miRNA levels (see Table 1).

The first study of a circulating miRNA profile in liver injury was conducted by Wang et al. [9]. The authors reported that two liver-enriched miRNAs (miR-122 and miR-192) were observed to be reliable serum biomarkers of acetaminophen-induced acute liver injury in mouse plasma in a dose-dependent and exposure duration-dependent manner, which paralleled that of ALT and caused histopathological changes in the liver. Moreover, these miRNAs were detected earlier than ALT and at lower doses, indicating greater sensitivity, and this change was more specific for viral-, alcohol-, and chemical-induced liver injury than for other organ damage, and was a more stable and reliable biomarker [41]. ALT and AST have also been shown to be increased in extrahepatic injury such as muscle damage or cardiac injury [38, 42]. Both of these parameters were increased in plasma samples from rats that had been treated with 2,3,5,6-tetramethyl-*p*-phenylenediamine (a skeletal muscle toxicant), although no hepatocellular degeneration or necrosis was observed. In the same plasma samples, levels of miR-133a, but not miR-122, were significantly elevated (more than 500-fold) when compared with levels in plasma samples from control rats [43]. In contrast, an approximately 6,000-fold increase in miR-122 and only a minimal increase in miR-133a (approximately 10-fold) was observed in rats treated with the liver toxicant trichlorobromomethane, indicating that miR-122 and miR-133a in plasma could be injured-tissue–distinguishable markers and clearly relative to ALT and AST. Interestingly, the specificity of serum miR-122 for acetaminophen-induced acute liver injury in humans was also examined in a heterogeneous group of patients with liver injury relative to comparator cohorts of healthy volunteers and patients with chronic proteinuric kidney disease [44]. That study showed that miR-122 levels in serum were raised and correlated with an existing biomarker of drug-induced liver injury, indicating that circulating miR-122 could be a novel and valuable diagnostic biomarker of human liver injury. In addition to drug-induced liver injury, several studies have reported that serum levels of miR-122 were increased in HBV- or HCV-induced liver injury [41, 45–47]. These data suggest that elevated circulating levels of miR-122 reflect liver injury independent of the cause of the injury. Therefore, pathogen-specific biomarkers are needed to identify the cause of human liver injury.

Yamamura et al. [48] reported that plasma miRNA profiles exhibited different patterns depending on the differentiating pathogenesis of acute and chronic liver injury, as well as hepatocellular injury, cholestasis, steatosis, steatohepatitis, and fibrosis in rat models, thus suggesting that plasma miRNA profiling could be useful for distinguishing the different types of liver injury when compared with conventional biomarkers, such as ALT and alkaline phosphatase (ALP). Interestingly, the state of circulating miRNAs in serum/plasma differed depending on the type of liver injury. Circulating miRNAs including miR-122 and miR-155 were predominantly associated with the exosome-rich fraction in alcoholic liver disease, whereas these miRNAs were present in the protein-rich fraction in drug-

Table 1 Tissue injury-associated microRNAs (miRNAs) in blood or urine

Injured tissue	Toxicants/diseases	Upregulated miRNAs	Body fluid	Species	References
Liver	Acetaminophen	miR-122, -192	Plasma	Mouse	[9]
Liver	Acetaminophen	miR-122, 146a, -155	Plasma (protein-rich fraction)	Mouse	[49]
Liver	Cytidine-phosphate-guanosine, lipopolysaccharide	miR-122, 146a, -155	Plasma (exosome-rich fraction)	Mouse	[49]
Liver	Ethanol	miR-122, -155	Plasma (exosome-rich fraction)	Mouse	[49]
Liver	Trichlorobromomethane	miR-122	Plasma	Rat	[43]
Liver	Acetaminophen	miR-122	Plasma	Human	[44]
Liver	Acetaminophen	miR-20b-3p, -34c*, -185, -291a-5p, -296, 330*, -433, -434, -484, -664	Urine	Rat	[50]
Liver	Hepatitis B, hepatitis C	miR-122	Plasma	Human	[41, 45–47]
Heart	Isoproterenol	miR-208	Plasma	Rat	[55]
Heart	Ischemic preconditioning, ischemia/reperfusion	miR-1	Plasma	Rat	[56]
Heart	Acute myocardial infarction[a]	miR-1	Urine	Rat	[57]
Heart	Acute myocardial infarction	miR-133a/b	Plasma	Human	[58–61]
Heart	Acute myocardial infarction	miR-499	Plasma	Human	[59, 60, 62]
Heart	Acute coronary syndrome	miR-1/-21/-499[b]	Plasma	Human	[63]

[a] Acute myocardial infarction induced by left anterior descending coronary artery ligation

[b] Combination use of the three miRNAs

induced liver injury [49]. These data indicated that extracellular distribution of miRNAs is distinct under different pathological conditions—for example, severe and rapid damage or mild and slower damage—in the liver.

Use of urine samples to detect miRNA as a biomarker could also be useful. Yang et al. [50] reported that specific miRNA profiles in urine were identified in acetaminophen- or carbon tetrachloride-induced liver injury rats. Ten miRNAs (miR-20b-3p, -34c*, -185, -291a-5p, -296, -330*, -433, -434, -484, and -664) were commonly increased by treatment with both acetaminophen and carbon tetrachloride in this model. Interestingly, the alteration pattern in urine reflected that in the liver, indicating that patterns of urinary miRNA hold promise as a good biomarker of hepatotoxicant-induced liver injury.

3 Use of Circulating miRNAs as Biomarkers of Safety for Assessment of Cardiovascular Toxicity

Cardiac safety biomarkers that translate from drug discovery through preclinical to clinical development and into the market are also necessary. Like hepatotoxicity, cardiotoxicity is an important cause of compound attrition in preclinical and clinical development. Cardiovascular toxicity accounted for 9% of withdrawals of prescription drugs from the worldwide pharmaceutical market from 1960 to 1999 [51]. In the cardiac field, biomarkers such as cardiac myoglobin, creatine kinase-MB isoenzymes, and troponins are now routinely used for assessment of myocardial injury [52]. Unfortunately, many of these markers have reduced sensitivity or less specificity, or do not allow timely diagnosis. Therefore, a multiple biomarker strategy may circumvent these limitations by adding accuracy and predictive power.

A recent report has suggested that serum levels of cardiac-expressed miRNAs react to cardiac injury in a manner similar to that of cardiac enzymes (Table 1). Most previous studies have focused on four miRNAs (miR-1, miR-133a/b, miR-208, and miR-499) as biomarkers of cardiac injury. Of these, miR-208 is expressed exclusively in the heart; the other miRNAs are expressed in both heart and skeletal muscle in humans and rats [53]. The first study of circulating miRNA in plasma in myocardial injury was